

Journal Pre-proof

Multi-performance experimental assessment of autogenous and crystalline admixture-stimulated self-healing in UHPFRCCs: Validation and reliability analysis through an inter-laboratory study

Francesco Lo Monte, Lamija Repesa, Didier Snoeck, Hesam Doostkami, Marta Roig-Flores, Sam J.P. Jackson, Ana Blanco Alvarez, Milena Nasner, Ruben Paul Borg, Christof Schröfl, Mercedes Giménez, Maria Cruz Alonso, Pedro Serna Ros, Nele De Belie, Liberato Ferrara

PII: S0958-9465(23)00389-X

DOI: <https://doi.org/10.1016/j.cemconcomp.2023.105315>

Reference: CECO 105315

To appear in: *Cement and Concrete Composites*

Received Date: 12 June 2023

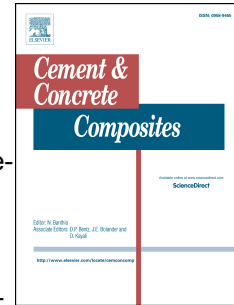
Revised Date: 29 September 2023

Accepted Date: 4 October 2023

Please cite this article as: F. Lo Monte, L. Repesa, D. Snoeck, H. Doostkami, M. Roig-Flores, S.J.P. Jackson, A.B. Alvarez, M. Nasner, R.P. Borg, C. Schröfl, M. Giménez, M.C. Alonso, P.S. Ros, N. De Belie, L. Ferrara, Multi-performance experimental assessment of autogenous and crystalline admixture-stimulated self-healing in UHPFRCCs: Validation and reliability analysis through an inter-laboratory study, *Cement and Concrete Composites* (2023), doi: <https://doi.org/10.1016/j.cemconcomp.2023.105315>.

This is a PDF file of an article that has undergone enhancements after acceptance, such as the addition of a cover page and metadata, and formatting for readability, but it is not yet the definitive version of record. This version will undergo additional copyediting, typesetting and review before it is published in its final form, but we are providing this version to give early visibility of the article. Please note that, during the production process, errors may be discovered which could affect the content, and all legal disclaimers that apply to the journal pertain.

© 2023 Published by Elsevier Ltd.



Multi-Performance Experimental Assessment of Autogenous and Crystalline Admixture-Stimulated Self-Healing in UHPFRCCs: Validation and Reliability Analysis through an Inter-Laboratory Study

Francesco Lo Monte¹, Lamija Repesa¹, Didier Snoeck^{2,3}, Hesam Doostkami⁴, Marta Roig-Flores^{4,9}, Sam J.P. Jackson⁵, Ana Blanco Alvarez⁵, Milena Nasner⁶, Ruben Paul Borg⁶, Christof Schröfl⁷, Mercedes Giménez⁸, Maria Cruz Alonso⁸, Pedro Serna Ros⁴, Nele De Belie³ and Liberato Ferrara¹

¹ *Department of Civil and Environmental Engineering, Politecnico di Milano (Italy)*

² *BATir, École Polytechnique de Bruxelles, Université Libre de Bruxelles (Belgium)*

³ *Department of Structural Engineering and Building Materials, Ghent University (Belgium)*

⁴ *Concrete Science and Technology Institute (ICITECH), Universitat Politècnica de Valencia (Spain)*

⁵ *School of Architecture, Building and Civil Engineering, Loughborough University (UK)*

⁶ *Faculty for the Built Environment, University of Malta (Malta)*

⁷ *Institute of Construction Materials, Technische Universität Dresden (Germany)*

⁸ *Institute of Construction Science Eduardo Torroja, CSIC (Spain)*

⁹ *Dep. of Mechanical Engineering and Construction, Universitat Jaume I (Spain)*

ABSTRACT. The huge benefits brought by the use of Ultra High-Performance Fibre-Reinforced Cementitious Composites (UHPFRCCs) include their high “intrinsic” durability, which is guaranteed by (1) the compact microstructure and (2) the positive interaction between stable multiple-cracking response and autogenous self-healing capability. Hence, self-healing capability must be properly characterized addressing different performances, thus providing all the tools for completely exploiting such large potential. Within this context, the need is clear for a well-established protocol for self-healing characterization. To this end, in the framework of the Cost Action CA15202 SARCOS, six Round Robin Tests involving 30 partners all around Europe were launched addressing different materials, spanning from ordinary concrete to UHPFRCC, and employing different self-healing technologies. In this paper, the tailored experimental methodology is presented and discussed for the specific case of autogenous and crystalline-admixture stimulated healing of UHPFRCC, starting from the comparison of the results from seven different laboratories. The methodology is based on chloride penetration and water permeability tests in cracked disks together with flexural tests on small beams. The latter ones are specifically aimed at assessing the flexural performance recovery of UHPFRCCs, which stands as their signature design “parameter” according to the most recent internationally recognized design approaches. This multi-fold test approach allows to address both inherent durability properties, such as through-crack chloride penetration and apparent water permeability, and more structural/mechanical aspects, such as flexural strength and stiffness.

KEYWORDS: Self-healing, crystalline admixtures, durability, UHPFRCC, inter-laboratory study.

1. INTRODUCTION

The study of concrete self-healing processes and technologies has come to a significant scientific maturity thanks to a relevant number of national and international projects devoted to the topic [1-9] and several large scale and in-situ real applications [10-20].

The state of the art has highlighted that self-healing can represent a powerful resource in the concrete construction industry to rely on more durable and longer lasting structures [21-25], thus also increasing the sustainability of the construction value chain [26-31]. However, even though a great potential hides behind the full exploitation of self-healing, a standard performance assessment framework has not been defined yet. In particular, standardized test methodologies are needed to quantitatively assess the efficiency of a particular technology with reference to the special performance requirement [32,33].

This highlights the demand for the formulation and validation of a comprehensive approach allowing to quantify the benefits of self-healing, in terms of recovery in both durability and mechanical performances, within a practitioner-friendly framework. Such an assessment should be based on reliably and robustly measureable parameters, which require standardized approaches for being monitored and which can be incorporated into durability-based design approaches [34,35]. Furthermore, not only the un-cracked condition has to be entailed, but also the cracked state of the material [10,36], since, as a matter of fact, it represents the most common condition in real structural service scenarios. Such structured approach could pave the way to a new role for self-healing as a clear-defined capability and no more as a mere bonus in civil structure and infrastructure engineering applications, thus translating into a technological and economical resource [37]. In this regard, the first effort should address the definition of key performance parameters on the base of which healing-induced property-recovery has to be sought, achieved and measured. This view comes from the main principle that self-healing cannot be comprehensively described by one parameter only (and thus assessed by a single experimental test), since concrete performance entails a set of properties which have a different role depending on the specific structural application.

Looking at the literature on the topic, healing is usually assessed (1) through visual evidence of crack closure (this being appropriately referred to as *crack self-sealing* or *surface crack closure*) or (2) through the recovery of durability-related parameters (such as water capillary absorption, water permeability and chloride diffusion) [38-49]. All the mentioned parameters directly refer to durability, since reduced values result into slower penetration in concrete of aggressive agents and into a slower structural degradation.

Among the influencing aspects in the definition of the assessment framework for self-healing capability, it can be mentioned (1) the type of cementitious material under investigation, (2) the related self-healing technology and (3) the intended final scenario. In a first step, this means distinguishing between Normal-Strength Concrete (NSC) and Ultra High-Performance Fibre-Reinforced Cementitious Composite

1 (UHPFRCC). In the former case, the tension (cracked) region is meant only to provide protection to the
2 reinforcement and concrete itself against the penetration of aggressive agents, while in the latter, the
3 tension (micro-cracked) region sizably contributes to the overall mechanical response.

4 UHPFRCC, in fact, is characterized by far lower values of durability-related parameters thanks to its
5 compact microstructure and by the ability to spread an otherwise localized crack into a series of thin and
6 tightly spaced multiple cracks. This latter condition is largely positive for UHPFRCC, thanks to the inborn
7 self-healing conduciveness of a narrow crack. In addition, self-healing processes are enhanced by the
8 peculiar mixture composition characterized by high cement and binder contents and low water/binder
9 ratios [50-52], which both provide significant amounts of anhydrous particles for delayed hydration.

10 The stable multiple cracking response in bending (deflection-hardening behaviour) and/or in tension
11 (strain-hardening behaviour) relies on the bridge-effect provided by structural fibres (metallic, poly-
12 meric or organic ones [53]). The role of fibres can be defined through a micromechanical approach
13 balancing crack tip toughness and fibre pull-out energy, with benefits for durability (as highlighted
14 before) and increased load bearing capacity [54,55].

15 In order to properly tackle the twofold advantage brought in by UHPFRCC, the assessment of the
16 healing-induced recovery of the material should address durability/transport properties as well as the
17 mechanical performance, which depends on crack closure and healing-induced improvement in the
18 fibre-matrix interface [56]. Both durability and mechanical response guarantee the stability over time
19 of the structural response in the intended scenario. This makes evident that self-healing assessment
20 should be based on a multiplicity of tests [57].

21 In order to discuss, in terms of repeatability and consistency, a multi-parameter methodology for self-
22 healing assessment in UHPFRCC [48], a Round Robin Test has been launched involving seven dif-
23 ferent laboratories. It is worth noting that this is one out of six Round Robin Tests launched in the
24 same period focusing on 6 different materials and/or self-healing technologies [48,58-62] (as sum-
25 marized in Table 1) organized under the umbrella of the COST Action CA15202 SARCOS [5] (Self-
26 healing As prevention Repair of COncrete Structures).

27 The Round Robin Test on UHPFRCC (RRT4 in Table 1) has involved Politecnico di Milano – PoliMi
28 (Italy), Ghent University – UGent (Belgium), Universitat Politècnica de València – UPV (Spain),
29 Loughborough University – LU (UK), University of Malta – UoM (Malta), Technische Universitaet
30 Dresden – TUD (Germany), and Institute of Construction Science Eduardo Torroja – CSIC (Spain).

31 The cementitious materials investigated in RRT4 were developed within the Horizon 2020
32 ReSHEALience project (Rethinking coastal defence and Green-energy Service infrastructures
33 through enHancEd-durAbiLity high-performance cement-based materials) [8,35,49,54,55,57] and
34 were employed for the construction of one of the project full-scale demonstrators, namely a tank
35 containing geothermal water and serving cooling towers in a geothermal power plant.

Table 1. Round Robin Tests campaign organized within the COST Action CA15202 SARCOS.

	Object		RRT Leader
RRT1	Concrete with mineral additions	[58]	Aristotele University of Technology
RRT2	Concrete with micro-encapsulated additions	[59]	University of Cambridge
RRT3	Concrete with crystalline admixture	[60]	Universitat Politecnica de Valencia
RRT4	UHPFRCC with crystalline admixture	[48]	Politecnico di Milano
RRT5	Concrete with macrocapsules filled with polyurethane	[61]	Ghent University
RRT6	Concrete with encapsulated bacteria	[62]	Technical University of Delft

The data set collected via this inter-laboratory test will also form the basis for further analyses within the framework of the MSCA-ITN SMARTINCS (Self-Healing, Multifunction, Advanced Repair Technologies in Cementitious Systems).

In the multi-test experimental procedure described in the next sections, self-healing is tackled from the point of view of both durability (in terms of transport properties) and mechanical performance. This has been pursued via three different test setups: chloride penetration assessment on cracked disks, water permeability on cracked disks and repeated bending tests on small beams.

The approach allowed investigating different key parameters through “recovery indexes” expected to embrace the main features connected to self-healing, namely durability (intended in a performance-based design framework) and mechanical response. In particular, crack self-sealing capability has been monitored in all the three test types, while recovery in terms of resistance against chloride penetration and water permeability has been studied via tests on disks, and mechanical recovery has been surveyed through repeated bending tests on small beams.

2. MATERIALS AND EXPERIMENTAL PLAN

2.1. UHPFRCCs’ mixture design

The methodology for self-healing assessment has been evaluated by investigating two Ultra-High Performance Fibre-Reinforced Cementitious Composite (UHPFRCC) mixtures (see Table 2), differing only in the presence of crystalline admixture (Penetron Admix ®) as self-healing stimulator (the benefits of which have been investigated in [63-67]).

The volume fraction is about 19% for cement (c) and slag (s), 38% for sand (a), 20% for water (w) (thus resulting into a ratio c:s:a:w close to 1:1:2:1) and 1.5% for steel fibres. Fibres are characterized by a length of 20 mm and a diameter of 0.22 mm, while their amount has been studied in order to obtain a nearly strain-hardening response in tension [54,68].

The composition of the two mixtures is detailed in Table 2. The mixing protocol consisted in mixing all the dry constituents for about two minutes, afterwards adding water and then the superplasticizer. Finally, steel fibres were added, followed by further ten minutes of high-speed mixing. The obtained self-levelling consistency guaranteed a proper dispersion of the fibres.

Table 2. Mix design of UHPFRCC mixtures. (% v_f = volume fraction percentage)

Constituents in [kg/m ³]/[% v_f]	Without (w/o) CA	with (w) CA
Cement CEM I 52.5R	600 / 19	600 / 19
Slag	500 / 19	500 / 19
Water	200 / 20	200 / 20
Steel fibers Azichem Readymix 200®	120 / 1.5	120 / 1.5
Sand (0-2 mm)	982 / 38	982 / 38
Superplasticizer BASF Glenium ACE 300®	33 / 3.5	33 / 3.5
Crystalline admixtures (CA) Penetron Admix®	0.0 / 0.0	4.8 / 0.2

2.2. Testing procedures for self-healing assessment

Following the needs for a multi-performance assessment of self-healing, according to the principles described in the introduction, three tests have been proposed in order to encompass the main specific features to be recovered by the materials:

- 1) evaluation of self-healing through the evolution of chloride penetration in pre-cracked disks;
- 2) evaluation of self-healing through recovery of water permeability in pre-cracked disks;
- 3) evaluation of self-healing through recovery of mechanical response in four-point bending tests.

All tests are detailed in the next sections together with the description of specimen production, curing conditions and pre-conditioning.

2.2.1. Evolution of chloride penetration on disks

In each laboratory involved in the inter-laboratory study, chloride penetration has been assessed for each mixture on nine concrete disks $\text{Ø}100 \times 80$ mm, obtained by cutting three cylinders with dimensions $\text{Ø}100 \times 280$ mm.

For each of the two UHPFRCC mixtures, chloride diffusion has been evaluated after 1, 3 and 6 months of continuous immersion in water with 33 g/L of NaCl (amount determined in order to simulate a seawater environment), changing the curing bath every month.

At time 0, before immersing the samples in the chloride aqueous solution, six out of the nine concrete disks were *pre-cracked* by splitting up to the target residual crack opening of (100 ± 50) μm , measured after unloading. Such value of crack opening has been chosen since it represents an upper bound of the crack width which can be expected for UHPFRCC (even at high tensile strain regime), as demonstrated by the results regarding the tests on small beams reported in the following sections.

The test setup adopted by PoliMi is reported in Figure 1, where crack opening has been monitored during splitting by means of three transducers. Very similar tests setups have been adopted by the other labs, without any substantial difference. Just after pre-cracking, the lateral face and one of the two circular bases were made waterproof via the application of silicon and tape (blue lines in the scheme of Figure 2), thus to instate a mostly 1D water flux within the immersed disks.

Image analysis of cracks was performed just after *pre-cracking* at time 0 and at the 3 target healing periods (namely 1, 3 and 6 months after time 0) capturing three microscope images for each diametrical crack of the specimen. Then the average surface crack width has been calculated.

1 Finally, the *Index of Crack Sealing (ICS)* has been computed as described in Equation 1:

$$ICS [-] = 1 - \frac{w_i}{w_{i-1}} \quad (1)$$

2 In equation 1, w_i is the average crack width at the end of the healing period and w_{i-1} is the average
3 crack width at the beginning of the healing period. In particular, w_{i-1} is the average crack width just
4 after *pre-cracking* for chloride penetration and water permeability tests (since no re-cracking is per-
5 formed), while it is the average crack width just after previous *re-cracking* for bending tests on thin
6 beams (since re-cracking was performed at any healing duration).

7 At time 0 all the nine samples (6 pre-cracked and 3 un-cracked) were immersed in salt water. After-
8 wards, at each target period and for each mixture, chloride penetration was evaluated on two pre-
9 cracked samples and on one un-cracked sample, according to at least one of the two following alter-
10 natives: (1) $AgNO_3$ sprayed on the mid split surface (similar to [32,44,47,48]) or (2) chemical titration
11 (similar to [32,40,42,46,47,48]). For both methodologies, no further pre-conditioning has been im-
12 plemented. A very similar procedure has been extensively used in [47].

13 The first approach required the splitting of the disks in two halves with a fracture plane (dashed green
14 lines in Figure 2) orthogonal to the previous (initial) crack triggered at time 0. In this way, the surface
15 to be exposed to $AgNO_3$ contained the transverse section of the previous crack, thus allowing to
16 observe the influence of the crack in the diffusion of chlorides orthogonal to crack walls. As sketched
17 in magenta colour in Figure 2, sprayed silver nitrate highlighted the area with a significant content of
18 chloride. Such region is then quantified via two parameters, the normalized Chloride Penetration Aver-
19 age depth (CPA), and the Chloride Penetration Depth measured far from the crack tip (CPD), as re-
20 ported in Equations 2a and 2b:

$$CPA [mm] = \frac{\text{area of the region highlighted by } AgNO_3}{\text{diameter of the disk}} \quad (2a)$$

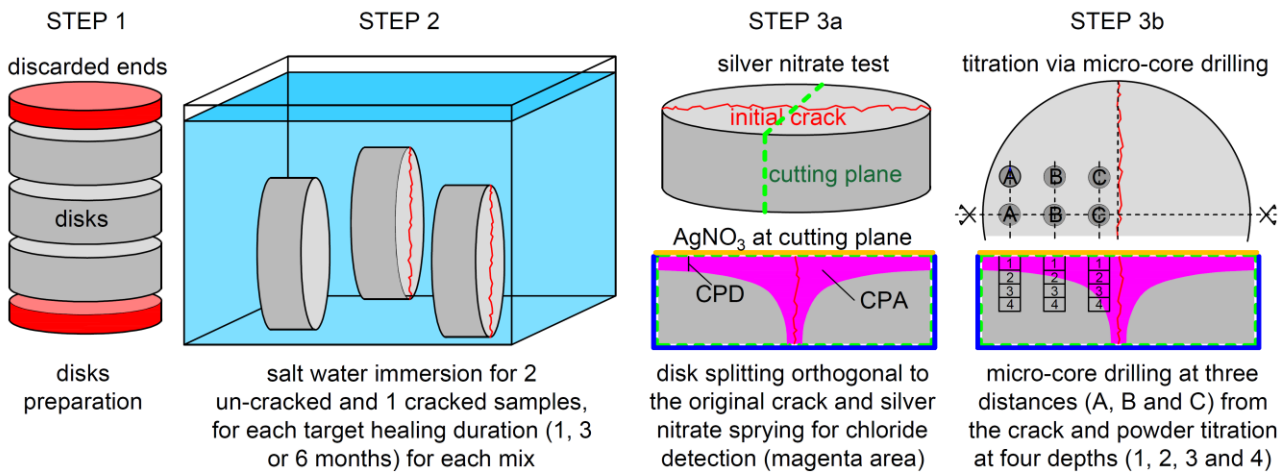
$$CPD [mm] = \text{depth of the region highlighted by } AgNO_3 \quad (2b)$$

21 CPD represents the chlorides penetration depth in un-cracked condition, while CPA takes into ac-
22 count the effect of the crack and thus of crack self-healing.

23 On the other hand, chemical titration was performed similarly as per BS EN 14629:2007 or
24 RILEM TC 178-TMC, according to a modified procedure conceived for this kind of materials (which
25 are characterized by a large amount of steel fibres).



Figure 1. Pre-cracking of disks as implemented at PoliMi for chloride penetration and permeability tests: (a) front and rear views of the set-up, (b) picture of a test and (c) qualitative loading curve.

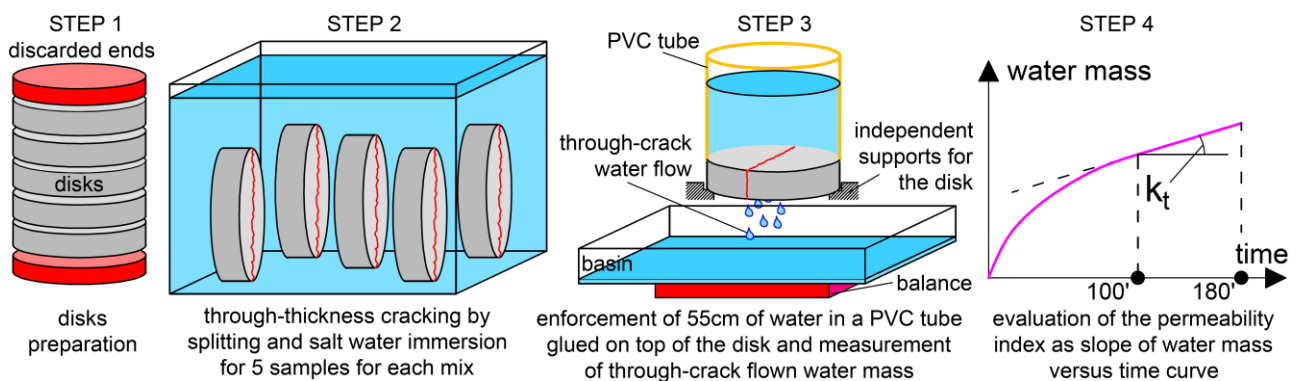


1
2 **Figure 2.** Disks cut from cylinders (step 1), then stored in water (step 2); cutting plane of a disk (green
3 dashed line) for AgNO₃ analysis and sketch of the area highlighted by AgNO₃ in the cutting surface (in
4 magenta colour) (step 3a) and sketch for titration via micro-core drilling (step 3b).

5 The procedure starts with drilling micro-cores with a diameter of 10 mm at three different positions
6 parallel to the diametrical crack and at three different distances orthogonal to it (A, B and C in Fig. 2).
7 As progressively drilled, the material in form of powder was separated at four different equally spaced
8 5mm depths, from 0 to 20 mm (1 to 4 in step 3b of Figure 2.). The 36 determinations obtained for each
9 specimen allowed to “reconstruct” the chloride penetration profiles. Since this latter approach has been
10 adopted by Lab1 and Lab4 only, and the results from the former can be already found in [48], this
11 second procedure is not further discussed in the present paper.

12 2.2.2. Water permeability recovery on disks

13 In each laboratory involved, water permeability test was carried out on each mixture on five concrete
14 disks with nominal dimensions Ø100 x 50 mm, obtained by cutting Ø100 x 280 mm cylinders (Fig-
15 ure 3). Each disk was *pre-cracked* by splitting at time 0 with a target residual crack width of
16 $(100 \pm 50) \mu\text{m}$ after unloading, with the same set-up shown for chloride penetration test (Figure 1).



17
18 **Figure 3.** Disks cut from cylinders (step 1), then stored in water (step 2); sketch of the water permeability test
19 set-up (step 3) and qualitative water mass flow versus time with the evaluation of the k_t coefficient (step 4)

1 Water permeability and crack image analysis were performed at time 0 (just after pre-cracking) and
 2 at the three healing periods, 1, 3 and 6 months from pre-cracking. The Index of Crack Sealing was
 3 calculated via image analysis at such target periods, in the same way described for chloride penetra-
 4 tion test (Equation 1). During the whole healing period, disks were kept immersed in tap water.

5 Water permeability test was performed by enforcing a water level of 55 cm above one of the two
 6 basis planes of the specimens. This was done by gluing PVC tubes on the top of the disks (orange in
 7 Figure 3) then filled with local tap water. During the test, the water mass flow through the thickness
 8 of the disks was monitored for 3 hours at different time intervals (namely, 0, 5, 10, 15, 20, 25, 30, 40,
 9 50, 60, 80, 100, 120, 150 and 180 min). A very similar testing procedure has been extensively imple-
 10 mented in [32,48,57,72], while water under pressure has been implemented in [69,70].

11 The indirect permeability index k_t was finally evaluated as the slope of flown-through water volume
 12 versus time curves in the range 100-180 min. Before performing the permeability test, the samples
 13 were preconditioned by 24 hours-drying at 60 °C.

14 The Index of Permeability Recovery (IPR) was then calculated as expressed in Equation 3:

$$IPR = 1 - \frac{k_t}{k_{t0}} \quad (3)$$

15 2.2.3. Strength and stiffness recovery on thin beams

16 The mechanical recovery triggered by self-healing was assessed via 4-point bending tests on thin
 17 beams with nominal dimensions of 25x100x500 mm³, with the aim of highlighting the multiple-
 18 cracking behaviour in the central region of the specimen. Such behaviour is representative for mate-
 19 rials with strain/deflection-hardening response and hardly sizable in 3-Point Bending.

20 During the test, the tensile deformation at the bottom side was monitored in order to measure the
 21 target residual strain after unloading. In Figure 4 the setup adopted at PoliMi is shown and very sim-
 22 ilar tests setups have been adopted by the other labs.

23 In order to assess any possible mechanical recovery as a function of the healing period, specimens
 24 were re-tested in bending at all the target periods, namely at time 0 (*pre-cracking*), and after 1, 3 and
 25 6 months (*re-cracking*) of healing. At each cracking step (both *pre-cracking* and *re-cracking*) an
 26 additional residual strain (after unloading) of 1‰ was attained.

27 At the end of pre-cracking via four-point bending (time 0), at least one crack at the bottom side of
 28 each specimen was recorded via digital microscope and image analysis was performed, in the same
 29 way discussed for disks. The same was done just before and just after any further re-cracking (at 1, 3
 30 and 6 months from time 0).

31 For each specimen, the total deformation was then obtained from consecutive σ -COD cycles, by
 32 translating the σ -COD curves along the x-axis in order to match the first point of the re-cracking (i)
 33 with the last point of the previous cracking (i-1), as shown in Figure 4c,d. This curve has then been
 34 compared to the reference one, namely the one related to an un-cracked specimen tested monoton-
 35 ically up to failure at the same time period with the same curing (at 1, 3 and 6 months from time 0).

This testing procedure has been developed in recent years with special reference to UHPFRCC [8,23,32,72,73] which, as mentioned above, is characterized by a signature tensile response usually leading to strain-hardening. This is the reason why 4-PBT is preferred, so to instate a multiple cracking regime which is representative in terms of crack pattern and crack width.

All the beams have been cast, cured and prepared at PoliMi and then shipped to the lab involved, ready to be pre-cracked. In each laboratory and for each mixture composition, 15 specimens were provided, 8 to be tested monotonically up to failure at each reference time (thus 2 specimens at time 0 and 2 after further 1, 3 and 6 months), and 7 to be pre-cracked at time 0, and then re-cracked at 1, 3 and 6 months for self-healing assessment.

Analysing the re-constructed curves of the pre-cracked/re-cracked specimens (as shown in Figure 4c) and comparing them with the reference one, it is possible to evaluate the mechanical recovery from the translated σ -COD curves by means of the following indexes:

- *Indexes of Stiffness Recovery (ISR)* according to Equations 4a and 4b:

$$ISR_0 [-] = \frac{K_c^i - K_s^0}{K_c^0 - K_s^0} \quad (4a)$$

$$ISR_{i-1} [-] = \frac{K_c^i - K_s^{i-1}}{K_c^{i-1} - K_s^{i-1}} \quad (4b)$$

ISR_0 represents the recovery with respect to the pre-cracking cycle (first loading cycle), while ISR_{i-1} represents the recovery with respect to the previous cracking cycle (either pre-cracking or re-cracking cycle). The two indexes are based on the evaluation of initial loading stiffness (K_c^0), first unloading stiffness (K_s^0), $(i-1)^{th}$ unloading stiffness (K_s^{i-1}) and i^{th} re-loading stiffness (K_c^i), as sketched in Figure 4c. ISR_0 and ISR_{i-1} are evaluated analysing singularly each reconstructed curve.

- *Index of Resistance Recovery (IRR)*, evaluated as expressed in Equation 5:

$$IRR[-] = 1 + \frac{\sigma_{recl,i} - \sigma_{ref,i}}{\sigma_{ref}} \quad (5)$$

The term $\sigma_{recl,i}$ is the stress at unloading at the i^{th} cracking cycle, $\sigma_{ref,i}$ is the stress in the reference curve in correspondence of the same strain of $\sigma_{recl,i}$, and σ_{ref} is the stress in the reference curve as sketched in Figure 4d. IRR is valuated comparing each reconstructed curve with the reference one.

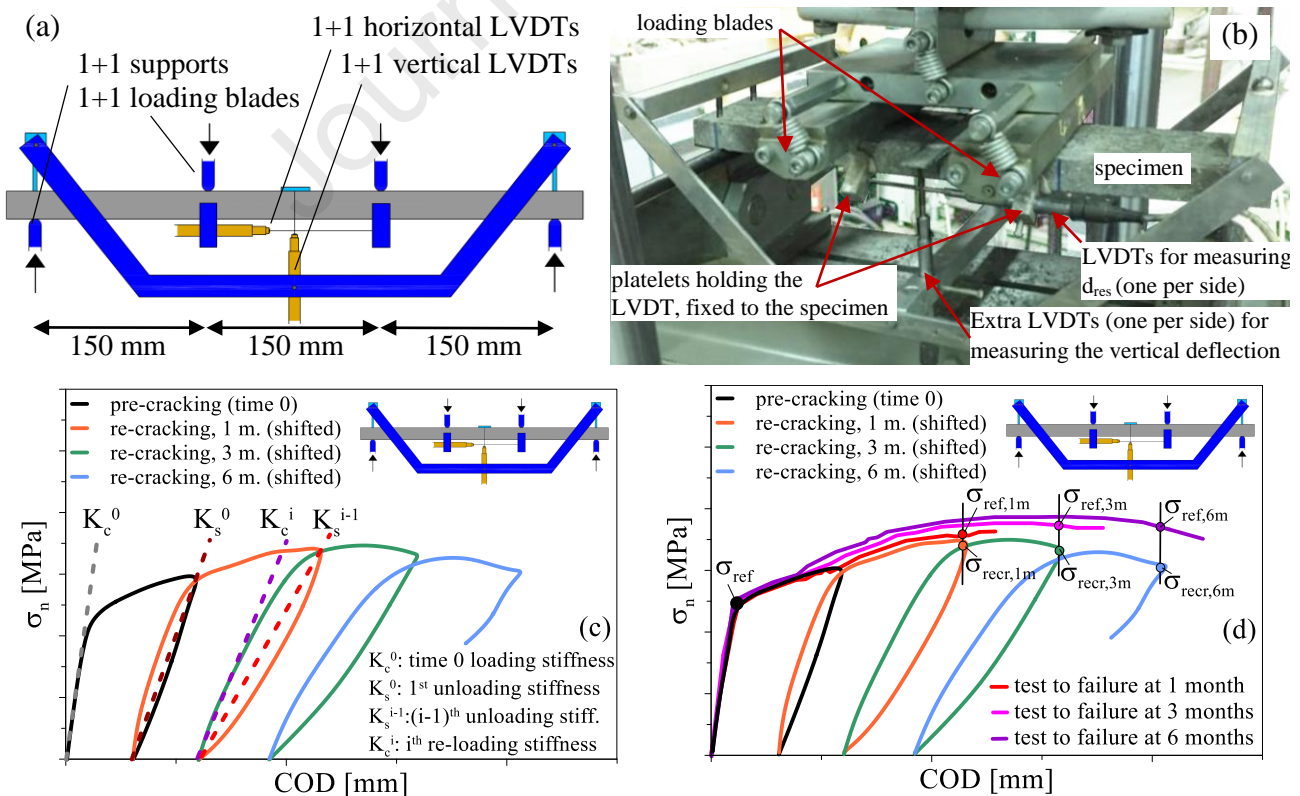
For all indexes, the value equal to 1 indicates complete recovery of the pristine performance of the specimen in its virgin/previous state. Crack visual inspection was also performed as described for the concrete disks in the previous section, thus allowing to evaluate the Index of Crack Sealing (ICS).

During the whole healing period, disks were kept immersed in tap water without any further pre-conditioning before flexural tests or crack image analysis.

2.3. Specimen production

All the specimens tested by the different laboratories involved in the Round Robin Test were cast and prepared at Politecnico di Milano at the end of 2019, respecting the above-mentioned mixing protocol. For each lab and for each of the two mixtures to be investigated, fifteen small beams (25 x 100 x

1 500 mm³) were produced, together with 4 cylinders (D x H = 100 x 280 mm).
 2 It is worth underlining that small beams were produced by casting concrete slabs with a nominal
 3 thickness of 25 mm and in-plane dimensions 500x1000 mm² that were then cut at PoliMi into 20
 4 beam specimens (100 mm wide and 500 mm long). Such procedure has been adopted since it guar-
 5 antees a better alignment of fibres as compared to the production of single specimens [54,57].
 6 On the other hand, 28 whole cylinders for each mixture have been prepared and cured at Polimi. Four
 7 cylinders per mixture were then shipped to each lab involved, the latter one being responsible for
 8 cutting the disks and for all the following procedures. By cutting nine 80 mm-thick disks (from 3 out
 9 of 4 cylinder) and five 50 mm-thick disks (from 1 out of 4 cylinder), for each mixture, samples for
 10 testing chloride penetration and water permeability were obtained, respectively.
 11 Table 3 shows the overall experimental program carried out in this study, while in Table 4, the experi-
 12 mental test type performed in each lab is reported. Finally, Table 5 shows the anonymous identification
 13 of the labs involved, together with the correspondent symbol adopted for data and results in Section 3.
 14 Due to CoVID-19 pandemic, specimens were shipped to the participating laboratories just after about
 15 one year from casting, in the second half of 2020. This, however, allowed to smooth down any de-
 16 layed hydration process within concrete, including latent hydraulicity of the slag.
 17 In the complete curing period, specimens were kept in a moist room, with a temperature of 20°C and
 18 R.H. of 90%.



19 **Figure 4.** Scheme (a) and picture (b) of the four-point bending test setup for pre-cracking and re-
 20 cracking of thin beams, and evaluation of (c) stiffness recovery and (d) strength recovery indexes

1 **Table 3.** Overall experimental program of RRT4

Month	Chlorides diffusion <i>9 specimens</i>	Water Permeability <i>5 specimens</i>	4-P bending in thin beams <i>15 specimens</i>
0	<ul style="list-style-type: none"> specimens 1 to 6 pre-cracked specimens 7 to 9 un-cracked 9 disks immersed in salt water 	<ul style="list-style-type: none"> 5 specimens pre-cracked 5 permeability tests done 	<ul style="list-style-type: none"> 7 specimens pre-cracked 2 specimens tested to failure 6 spec. un-cracked cured as cracked
1	<ul style="list-style-type: none"> spec. 1, 2, 7 split and titrated spec. 3 to 6, 8, 9 kept in salt water 	<ul style="list-style-type: none"> 5 specimens subjected to permeability test 	<ul style="list-style-type: none"> 7 specimens re-cracked 2 spec. un-cracked tested up to failure
3	<ul style="list-style-type: none"> spec. 3, 4, 8 split and titrated spec. 5, 6, 9 kept in salt water 	<ul style="list-style-type: none"> 5 specimens subjected to permeability test 	<ul style="list-style-type: none"> 7 specimens re-cracked 2 spec. un-cracked tested up to failure
6	<ul style="list-style-type: none"> spec. 5, 6, 9 split and titrated 	<ul style="list-style-type: none"> 5 specimens subjected to permeability test 	<ul style="list-style-type: none"> 7 specimens re-cracked 2 spec. un-cracked tested up to failure
healing storage	continuous immersion in salt water (with 33 g/L NaCl)	continuous immersion in tap water	continuous immersion in tap water
pre-conditioning	no preconditioning before cracking/splitting/titration	24 hours-drying at 60 °C before permeability test	no preconditioning before flexural testing

2 **Table 4.** Universities and Laboratories involved in Round Robin Test 4

	Chloride penetration	Water permeability	4PBT on thin beams
Polimi	X (titration + ICS)	X	X
UGent	X (silver nitr + ICS)	X	X
UPV	X (silver nitr + ICS)	X	X
LU	X (titration + ICS)	X	X
UoM	X (silver nitr + ICS)	X	-
TUD	X (ICS)	X	-
CSIC	-	X	-

3 **Table 5.** Anonymous identification of laboratories involved in Round Robin Test 4 and correspond-
4 ent symbol

	symbols in the plots	
	w/o admixt.	with admixt.
Lab 1	○	●
Lab 2	□	■
Lab 3	△	▲
Lab 4	◇	◆
Lab 5	+	+
Lab 6	*	*
Lab 7	▽	▼
Avg	●	●

5 **3. RESULTS AND DISCUSSION**6 **3.1. Chloride penetration test**

7 At the reference time durations for self-healing assessment, namely at 1, 3 and 6 months from time 0,
8 a triplet of disks (two of which pre-cracked at time 0 and one un-cracked) was split orthogonally to
9 the initial crack and then examined by means of silver nitrate sprayed on it (as sketched in Figure 2).

1 The region highlighted by silver nitrate is quantified via Chloride Penetration Average depth (CPA)
2 and Chloride Penetration Depth measured far from the crack tip (CPD).

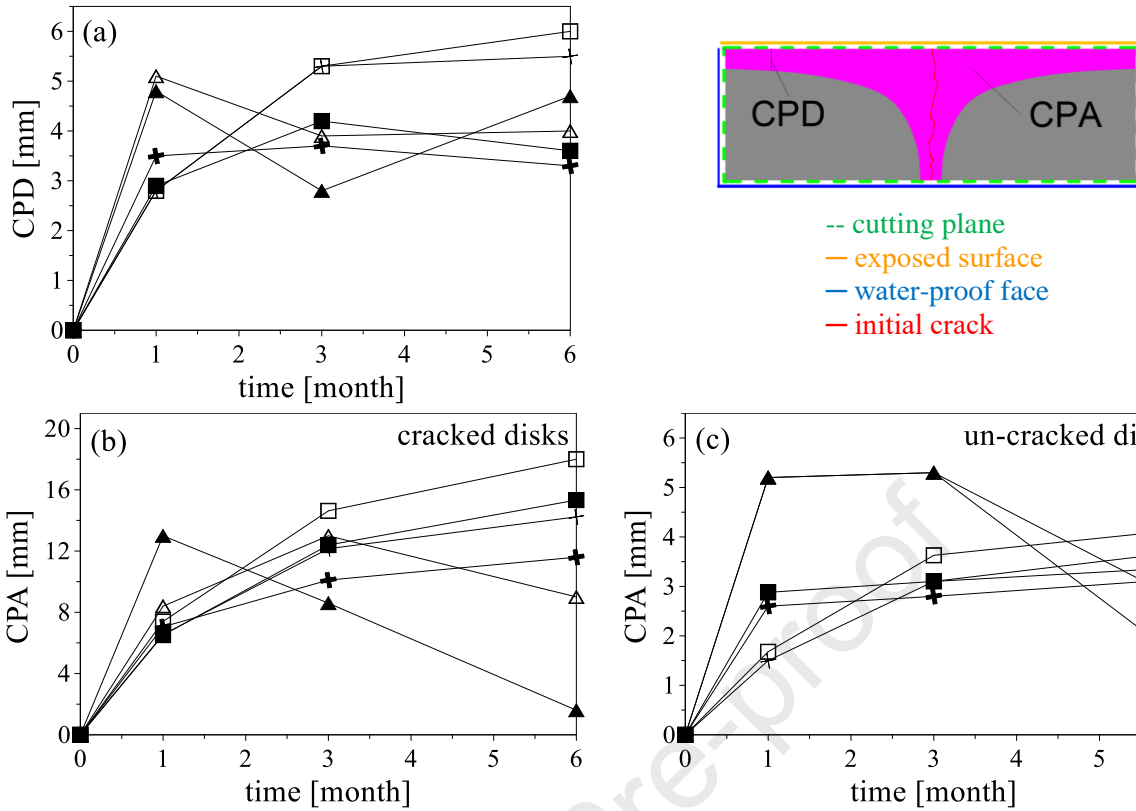
3 The average variation with time of CPD is reported in Figure 5a as a function of the healing period.
4 Cracked and un-cracked disks are considered together since CPD is evaluated far from the crack,
5 where its influence on the chloride penetration depth is negligible (thus no sizable difference is ex-
6 pected between cracked and un-cracked specimens). On the other hand, CPA average values are re-
7 ported in Figure 5b,c for each healing period differentiating between cracked and un-cracked disks.
8 Focusing on CPD, it can be observed that, over time, the chloride penetrates less deep into the spec-
9 imens with crystalline admixture thanks to the lower porosity of the matrix as fostered by the crystal-
10 line admixture [74]. It is worth noting that CPD and CPA in un-cracked specimens provide compa-
11 rable results (with all data comprised in the range 1.5-6.0 mm), since CPA in un-cracked specimen
12 represents the average penetration depth along the diameter.

13 The scattering among the results of the three laboratories involved is rather limited in the case of
14 CPD, while it is larger in the case of CPA. This is probably due to the influence of (a) the water-
15 tightness of the lateral faces which affects the penetration of chloride at the edges and of (b) the initial
16 crack width after pre-cracking (which is on average 127, 158 and 130 μm for Lab2, Lab3 and Lab5,
17 respectively, with standard deviation of 35, 95 and 52 μm , respectively).

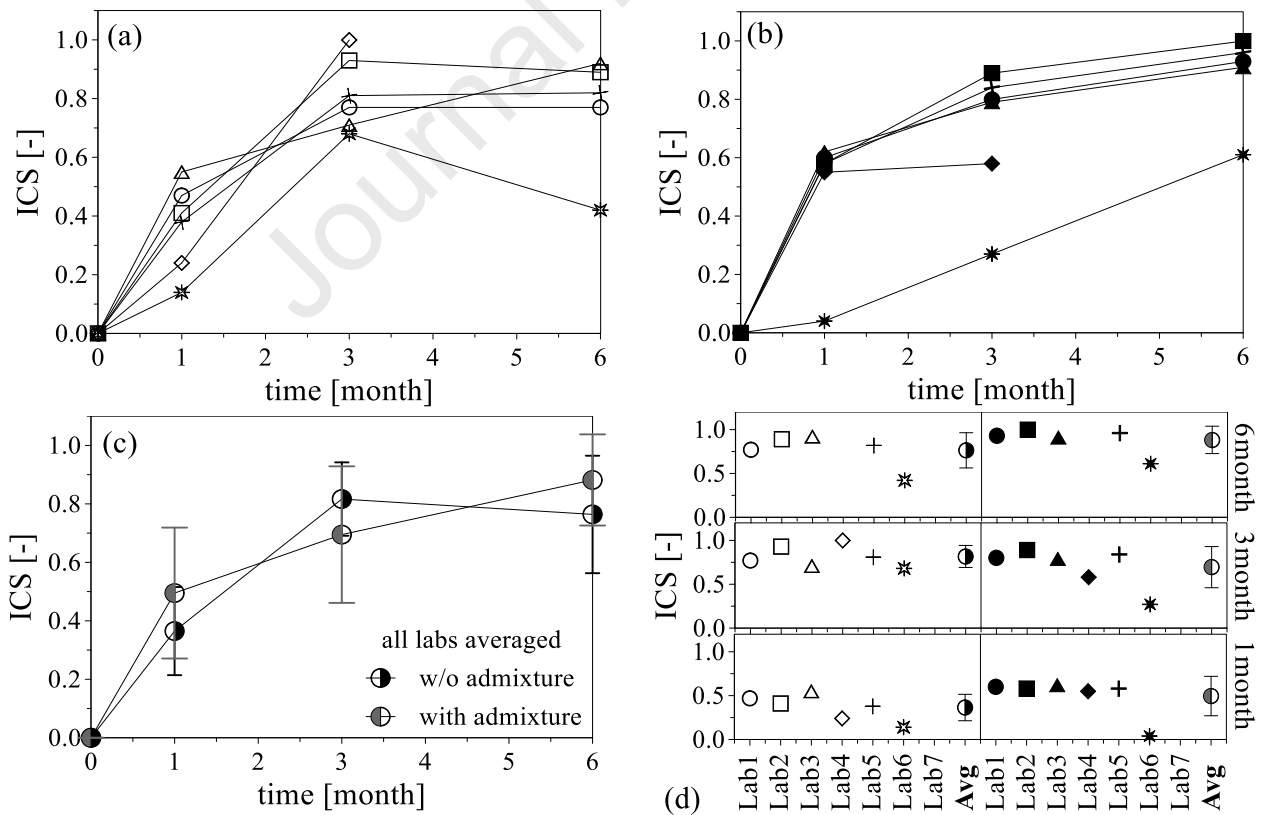
18 In all the cases, however, also CPA proves a slightly lower penetration of chlorides into the specimens
19 with crystalline admixture thanks to the lower initial porosity fostered by this admixture [74] and,
20 likely, also to a more effective crack sealing allowed by it. As expected, comparing cracked and un-
21 cracked specimens, it can be observed that CPA is much larger in the former case due to the presence
22 of cracks which allow a significant inlet of chlorides.

23 Regarding CPA for both cracked and un-cracked disks, the markedly different trend observed at Lab3
24 with respect to Lab2 and Lab5 in the range 3 to 6 months of healing has been object of investigation,
25 but a clear explanation has not been identified. Most of the disks used at Lab3 for the characterization
26 at 6 months belonged to the bottom part of the cylinders, where a slightly larger content of fibre and
27 a lower porosity is expected, this probably leading to lower values of chlorides penetration.

28 Further information can be obtained thanks to the titration as discussed in details in [48]. It was found
29 that after one-month exposure, in the mixture without crystalline admixture an immediate quite strong
30 penetration of chlorides throughout the crack depth was evident, whereas a sizably lower trend has
31 been measured for the mix with crystalline admixture. This is likely a consequence of a faster crack
32 sealing in the latter case. For prolonged exposure time up to six months, the penetration of chlorides
33 along the cracked plane continued, in this case the better crack sealing efficacy of the mixture with
34 crystalline admixture being instrumental at reducing the chloride content by about 20-25%.



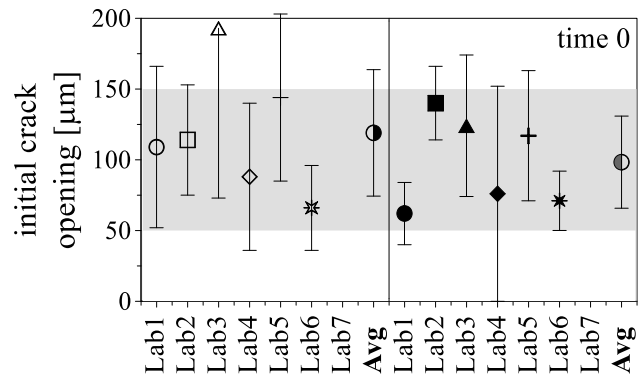
1 **Figure 5.** Average values of CPD for all disks (a) and of CPA for cracked disks (b) and un-cracked
 2 disks (c) as functions of self-healing time for the mixtures without and with crystalline admixture



3 **Figure 6.** ICS for the mixtures without (a,d) and with (b,d) admixture divided per participant, and
 4 values averaged among all the laboratories (c,d), from chloride penetration tests

1 **Table 6.** Average values (w_{avg}) and standard deviations (w_{σ}) of initial crack opening at time 0

	Without CA		With CA	
	w_{avg} [μm]	w_{σ} [μm]	w_{avg} [μm]	w_{σ} [μm]
Lab1	109	± 57	62	± 22
Lab2	114	± 39	140	± 26
Lab3	193	± 120	124	± 50
Lab4	88	± 52	76	± 76
Lab5	144	± 59	117	± 46
Lab6	66	± 30	71	± 21
Lab7	-	-	-	-
Avg	114	± 48	95	± 35



2 Regarding the values of ICS reported in Figure 6, among five of the six laboratories involved (Lab1,
 3 Lab2, Lab3, Lab4 and Lab5) a satisfactory agreement can be observed, both considering singularly
 4 each of the two mixtures, and comparing the trend going from the mixture with admixture to the mix
 5 without. In general, no significant difference between the mixes with or without CA can be observed.
 6 Table 6 shows the initial crack width (averaged for each mix among the 6 cracked specimens) without
 7 highlighting specific trends with respect to Figure 6.

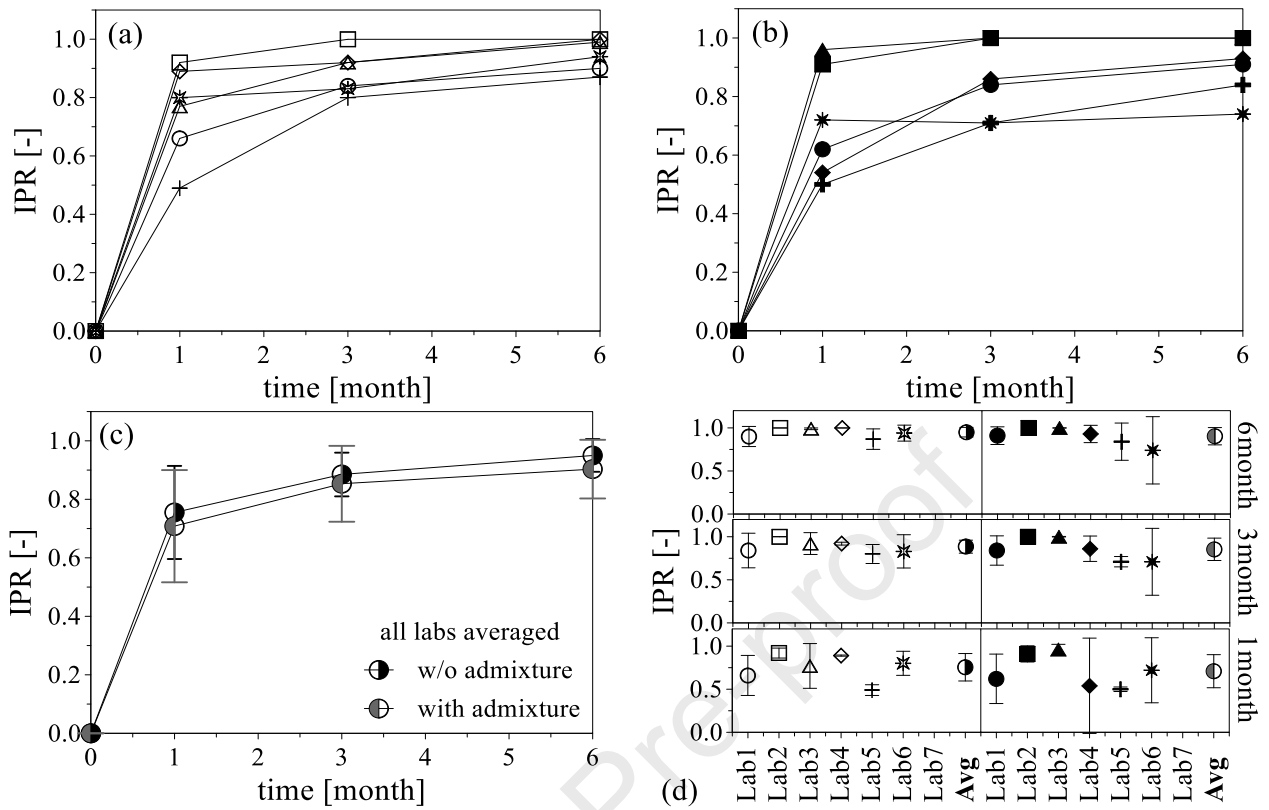
8 3.2. Water permeability test

9 Figures 7 and 8 show the values of the Indexes of Permeability Recovery (IPR) and of Crack Sealing
 10 (ICS), respectively, for the two investigated mixtures as functions of the healing time. The values of
 11 IPR and ICS plotted represents the average of data obtained from 5 disks, for each concrete mixture
 12 at every healing period. Figure 7a,b and Figure 8a,b report the results related to the mixture without
 13 and with admixture, respectively, for each participant, while Figure 7c and Figure 8c report the aver-
 14 age values considering all labs together.

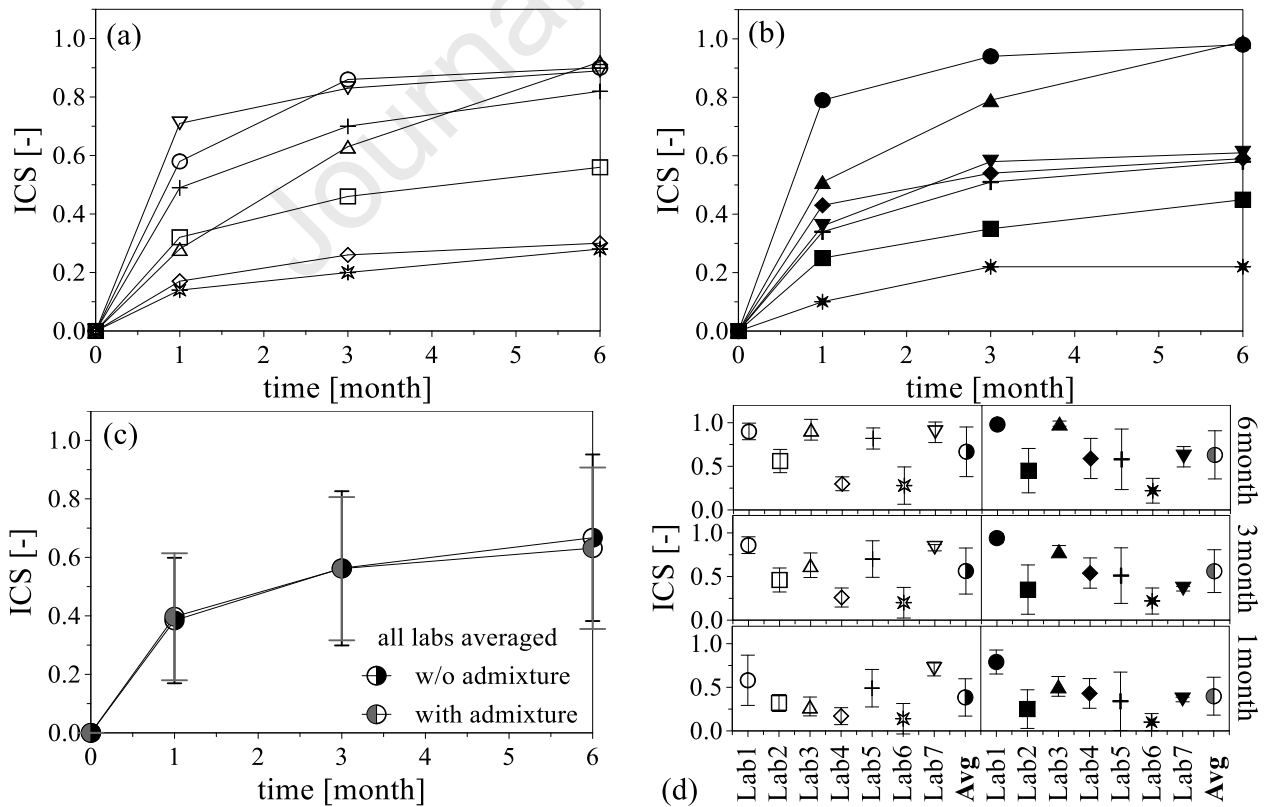
15 It can be observed that the scattering of the results among the laboratories is less evident in the case of
 16 IPR with respect to ICS, since, as also observed in [48,57], self-healing effectively affects water flow
 17 through very narrow cracks when a limited water pressure overhead is considered [69-72]. Nevertheless,
 18 the trend shown going from mixture without to mixture with admixture is not very clear, since, in general,
 19 the differences between the two species are rather limited. Averaging all data (Figure 7c), it appears that
 20 the introduction of crystalline admixture brings scant benefits in terms of water permeability recovery.

21 Similar consideration can be extended to ICS, since for Lab1, Lab3 and Lab4 crystalline admixture
 22 provides a slightly more efficient recovery, while the opposite is observed by Lab7. On the other
 23 hand, no significant difference between the two mixtures has been observed by Lab2, Lab5 and Lab6.
 24 Also in this case, averaging all data (Figure 8c), it appears that the introduction of crystalline admix-
 25 ture brings no evident benefit in terms of crack sealing. This can be ascribed to the fact that, in some
 26 cases (Lab1, Lab2 and Lab6), the obtained average crack openings fall within a range (50-100 μm)
 27 for which the autogenous healing capacity of UHPFRCC was systematically and reliably demon-
 28 strated able to close the crack, thus shadowing any possible effect of the stimulation by means of

1 crystalline admixtures. This autogenous healing can occur up to several years of age [75].



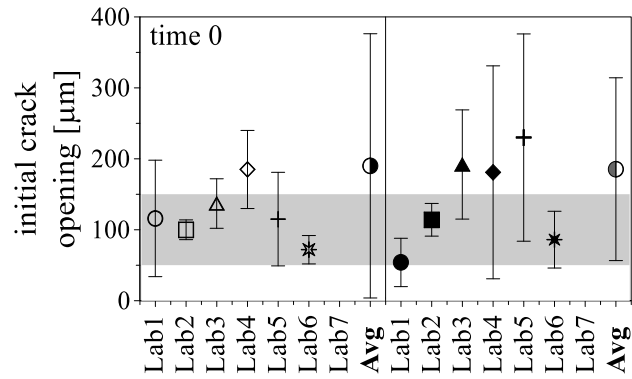
2 **Figure 7.** IPR for the mixtures without (a,d) and with (b,d) admixture divided per participant, and
 3 values averaged among all participants (c,d)



4 **Figure 8.** ICS for the mixtures without (a,d) and with (b,d) admixture divided per participant, and
 5 values averaged among all participants (c,d)

1 **Table 7.** Average values and standard deviations of initial crack opening at time 0 (w_{avg} and w_{σ})

	Without CA		With CA	
	w_{avg} [μm]	w_{σ} [μm]	w_{avg} [μm]	w_{σ} [μm]
Lab1	116	± 82	54	± 34
Lab2	100	± 14	114	± 23
Lab3	137	± 35	192	± 77
Lab4	185	± 55	181	± 150
Lab5	115	± 66	230	± 146
Lab6	72	± 20	86	± 40
Lab7	605	± 435	441	± 436
Avg	190	± 186	185	± 129



2 Table 7 shows the initial crack width (averaged for each mix among the 5 cracked specimens).

3 3.3 Flexural tests of thin beams: mechanical recovery and crack sealing indexes

4 As above mentioned, in the quantification of the healing-induced recovery on the mechanical perfor-
 5 mance, four-point bending test was preferred over three-point bending since the former allows to
 6 observe the multiple cracking stage. This, in fact, is the typical response for such kind of cementitious
 7 materials thanks to the activation of the crack-bridging effect of steel fibres. The central region of the
 8 specimens bordered by the two loading blades experiences constant bending moment and several
 9 cracks form in this region (which can be meant as characterized by a constant smeared tensile strain).
 10 This aspect is rather important since it allows to define reference thresholds in terms of strain, rather
 11 than in terms of crack width, the latter not being known a priori in structural applications. An inter-
 12 esting range of values of tensile strain is 2.0-2.5‰ which comprises the nominal strain related to f_{R1k}
 13 and the characteristic yielding strain of common reinforcement bars. In particular, f_{R1k} is the reference
 14 residual strength of Fiber-Reinforced Concrete for serviceability conditions (as measured via 3-Point
 15 Bending Test) and it is equal to about 2.0‰. On the other hand, the characteristic yielding strain of
 16 reinforcement bars is equal to about 2.4‰ for the most used steel type in Europe (namely B500).
 17 In order to explore such range of tensile strain, the nominal residual value of 1‰ at each cracking
 18 stage was set in the test programme, thus obtaining 1‰ after initial pre-cracking at time 0 and 2 and
 19 3‰ after second (at 1 month) and third (at 3 months) re-cracking. Tensile deformation was measured
 20 in the tests at the bottom side of the specimen between the supports by displacement transducers
 21 across the whole central zone (see also [48]).

22 For a deeper understanding of the results reported in the following, the distribution of the crack width
 23 observed in the specimens after pre-cracking and after each re-cracking is shown in Figure 9. It plots
 24 the percentage of cracks versus the crack width, organized in crack width ranges of 10 μm , for the
 25 different observation periods.

26 The widest range of crack opening was experienced in the tests performed at Lab1, where cracks up
 27 to 90-100 μm were observed after the first pre-cracking. On the contrary, at Lab3 most of the cracks

1 belonged to the range 0-30 μm , while an intermediate condition can be highlighted for Lab2 and
2 Lab4. Looking at the medians, however, crack width varies from 0-10 μm (Lab3) to 30-40 μm (Lab1).
3 For chloride and permeability testing, a 100 μm wide crack was thus set as a target in the pre-cracking
4 phase, since it represents an upper bound for crack width in this kind of UHPFRCC.

5 The observed difference in median crack width can be ascribed to slightly inevitable variations among
6 the batches in terms of fibre distribution/orientation which can lead to differences in terms of average
7 distance among cracks (thus influencing the number of cracks and their average opening). These
8 differences in terms of initial crack width should be taken into account when discussing the results
9 regarding self-healing indexes.

10 Figure 10 shows the Index of Stiffness Recovery with respect to pre-cracking (ISR_0), differentiated
11 per each participant in Figure 10a,b, and averaging all the data in Figure 10c, for the mixtures without
12 and with admixture. The same scheme is followed in Figure 11 for the Index of Stiffness Recovery
13 with respect to previous re-cracking (ISR_{i-1}).

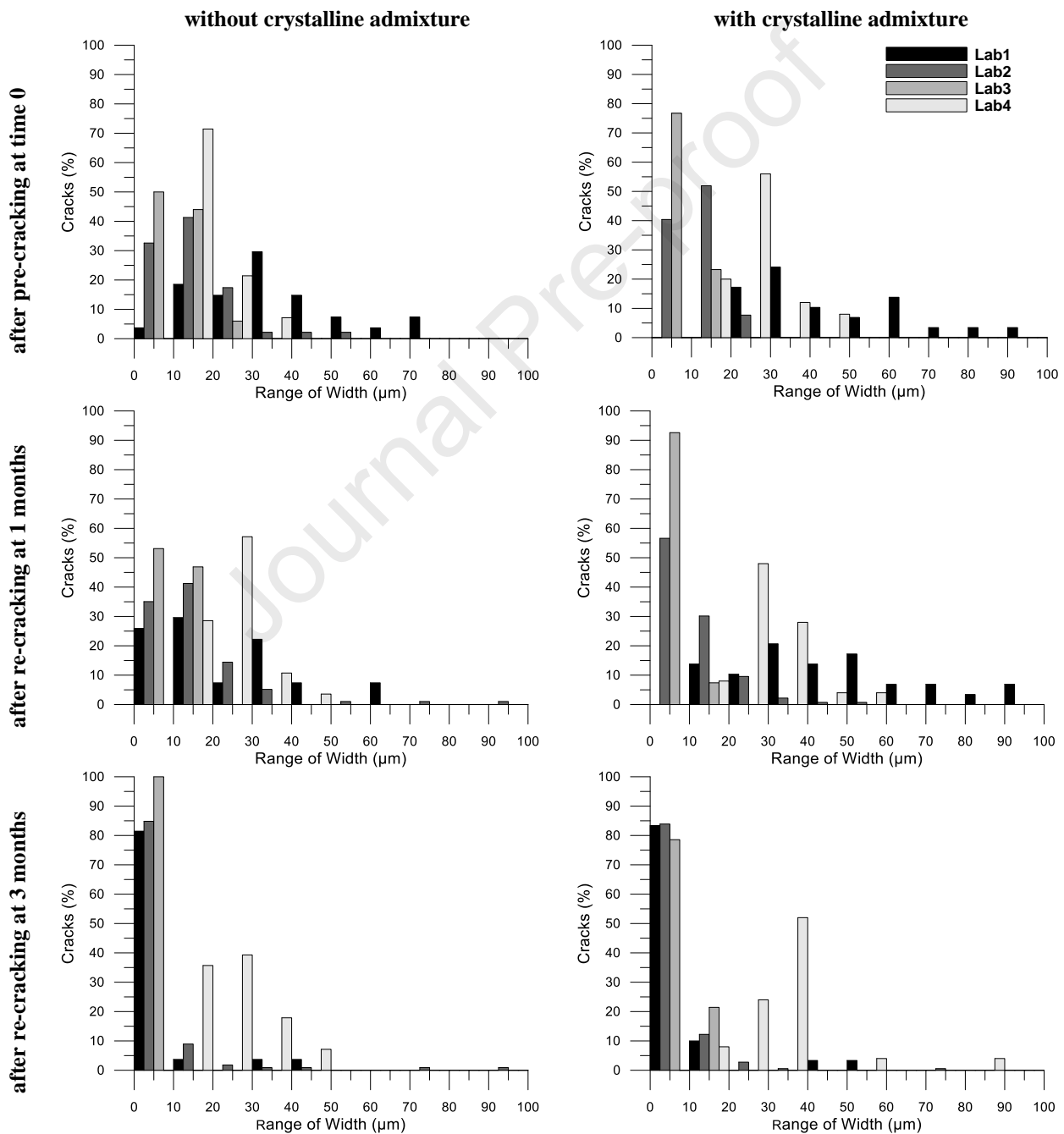
14 Focusing on the ISR_0 index, a rather good agreement can be observed for the results of Lab1 and
15 Lab2, whereas the results from Lab4 lead to much lower values (even though no evident differences
16 in the crack width distribution or curing conditions have been noticed). On the opposite, Lab3 ob-
17 served significantly higher values at 3 and 6 months of healing. This last outcome can be ascribed to
18 a preferential localization of fibres in the bottom part of the specimen (this being responsible for
19 initial cracks characterized by reduced interspace and narrow width), thus leading to a rather steep
20 slope in reloading curve for limited stress level (up to about 25% of tensile strength), with a conse-
21 quent higher observed recovery in terms of stiffness.

22 Considering the results from Lab1 and Lab2, crystalline admixture yields a more significant healing
23 for all the curing durations, while looking at the averaged values among all participants a clear trend
24 is not evident.

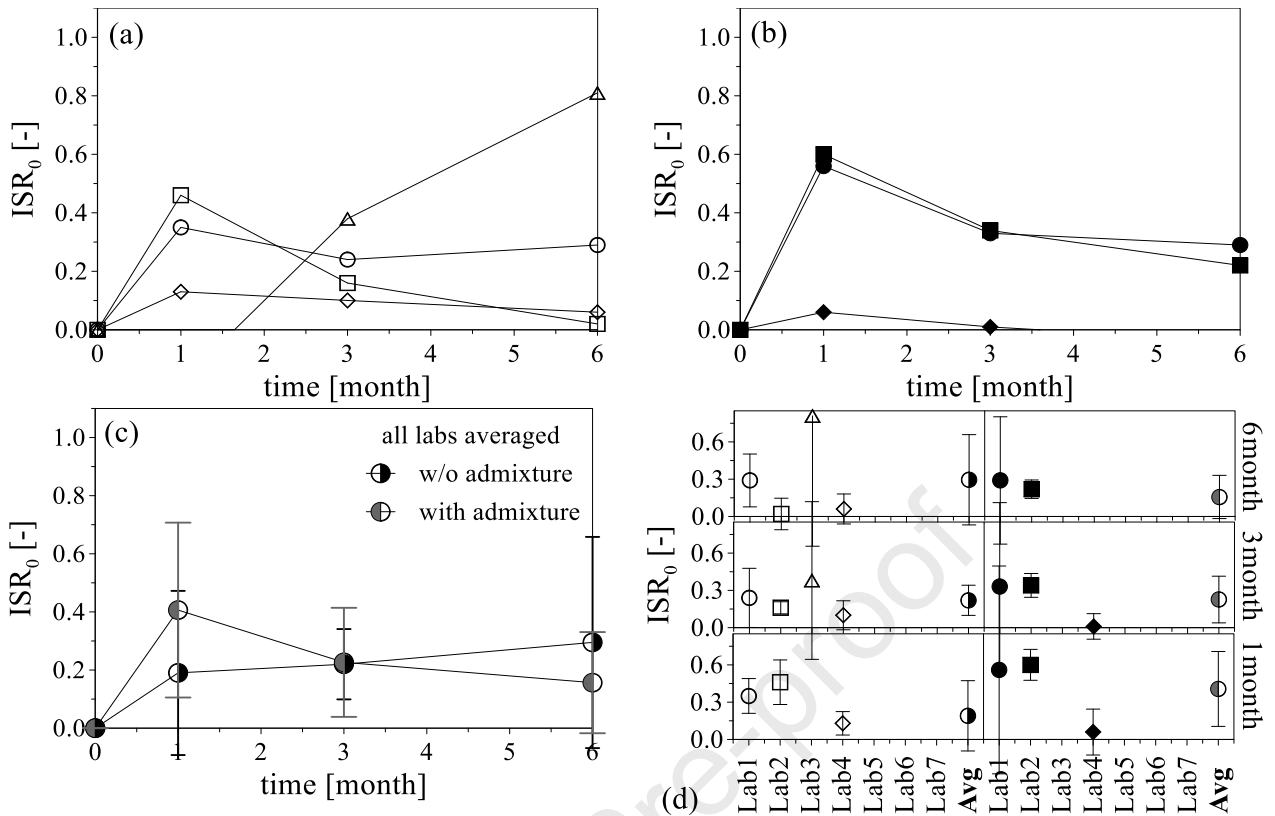
25 Very similar considerations can be made regarding ISR_{i-1} index, since Lab1 and Lab2 provide results
26 in good agreement, while Lab4 at 1 month provides lower values. On the contrary, Lab4 values at 3
27 and 6 months are more aligned with the other universities. Also in this case, considering the averaged
28 values among all participants, crystalline admixture appears to have no significant effect on the heal-
29 ing-induced recovery of the mechanical performance.

30 In order to conclude the analysis on the mechanical healing-related indexes, Figure 12 shows the
31 Index of Resistance Recovery (IRR), differentiating for each laboratory in Figure 12a,b, and averag-
32 ing all the data in Figure 12c, for the mixture without and with admixture. The results related to the
33 mixture without admixture are quite scattered, while for the mixture with admixture a higher repeat-
34 ability can be highlighted. It is interesting to observe that for Lab1 and Lab2, higher values of recov-
35 ery are observed for the mixture with crystalline admixture, while an opposite trend yields from the

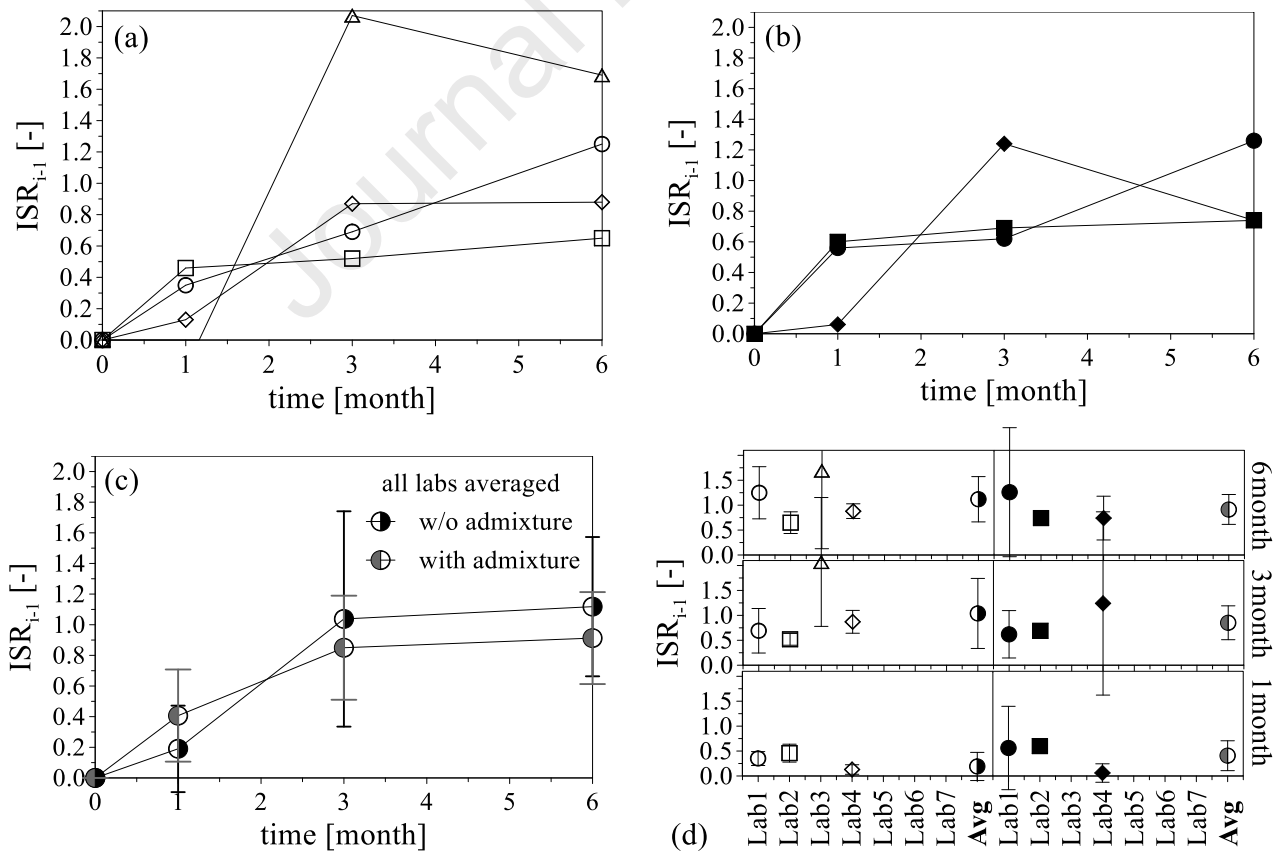
1 results by Lab3. Averaging all the results in Figure 12c, therefore, leads to similar performance of the
 2 mixtures with and without crystalline admixture.
 3 Finally, Figure 13 shows the index of crack sealing (ICS), differentiating for each laboratory in Fig-
 4 ure 13a,b, and averaging all the data in Figure 13c, for the mixture without and with admixture.
 5 It is worth noting that the dataset of cracks is much larger than in the case of the disks used for chloride
 6 penetration test and for permeability tests, since in each of the small beams subjected to bending test
 7 several cracks have been formed. It can be observed that the results of Lab1, Lab2 and Lab3 are in
 8 rather satisfactory agreement for both mixtures.



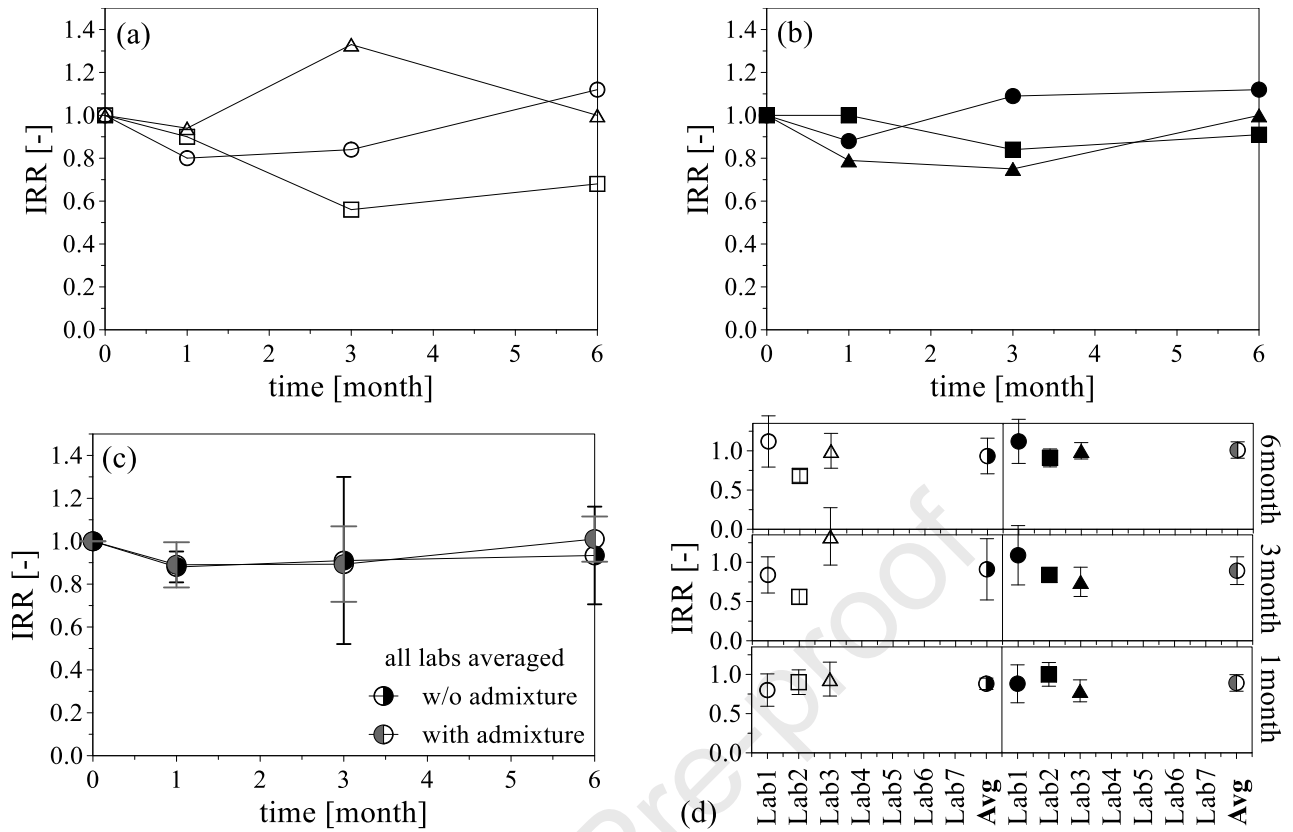
9 **Figure 9.** Crack width distribution at each cracking stage for mixture without and with admixture,
 10 differentiating among laboratories



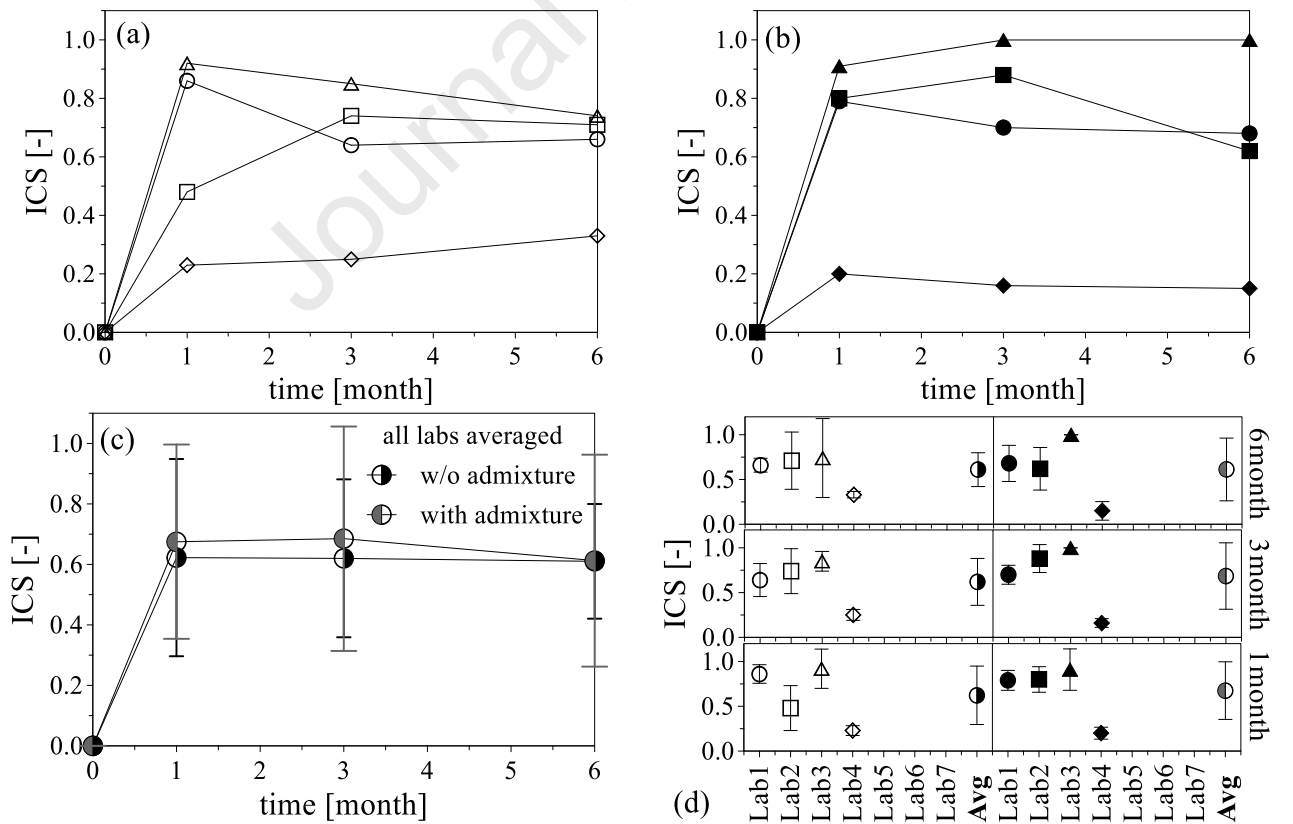
1 **Figure 10.** ISR_0 for the mixtures without (a,d) and with (b,d) admixture divided per laboratory, and values averaged among all the laboratories (c,d)
 2



3 **Figure 11.** ISR_{i-1} for the mixtures without (a,d) and with (b,d) admixture divided per laboratory, and values averaged among all the laboratories (c,d)
 4



1 **Figure 12.** IRR for the mixtures without (a,d) and with (b,d) admixture divided per laboratory, and
 2 values averaged among all the laboratories (c,d)



3 **Figure 13.** ICS for the mixtures without (a,d) and with (b,d) admixture divided per laboratory, and
 4 values averaged among all the laboratories (c,d)

5

1 On the opposite, far lower values of ICS have been assessed at Lab4 (even though no evident differ-
 2 ences in the crack width distribution or curing conditions were noticed) with a better performance
 3 provided by the mix without admixture. Averaging the data coming from all the laboratories, it can
 4 be seen that the differences between both mixtures is not significant also in the case of ICS.

5 As highlighted in the case of water permeability, the limited differences between the two mixtures can be
 6 ascribed to the fact that the autogenous healing capacity of UHPFRCC is rather effective, thus smoothing
 7 down any possible effect of the stimulation by means of crystalline admixtures (see also [48]).

8 3.4 Considerations about the consistency of self-healing indices

9 In Table 8 the averaged values μ of all the self-healing indexes are reported for the mixture without
 10 and with crystalline admixture together with the coefficient of variation $CoV = \sigma/\mu$ (the latter ex-
 11 pressed as a percentage). Average values and coefficients of variation have been calculated consid-
 12 ering the population of data represented by the set of average values from each laboratory.

13 Table 8 allows to preliminary assess the dispersion of the average data coming from different labor-
 14 atories. Coefficient of variation, in fact, has been also classified as - 1 - *very good* ($0 \leq Cov \leq 10\%$, dark
 15 green in the table), - 2 - *good* ($10 < Cov \leq 20\%$, green), - 3 - *acceptable* ($20 \leq Cov < 30\%$, light green), - 4 -
 16 *poor* ($30 < Cov \leq 40\%$, yellow), - 5 - *very poor* ($40 < Cov \leq 50\%$, orange), and - 6 - *unacceptable*
 17 ($Cov > 50\%$, red). Once assigned the class for each index, for all the healing periods and for the two
 18 mixtures, the average class associated to each of the 10 indexes has been calculated.

19 If the average class is in the ranges 1-2, the robustness of the index is considered *high*, if it is in the
 20 range 3-4, it is considered *medium*, otherwise it is considered *low* or *insufficient*. In the following, the
 21 robustness is considered *insufficient* if the average class is larger than 5.5. This corresponds to the
 22 case in which, in at least one half of the healing periods, the normalized standard deviation is larger
 23 than 50%. According to such approach the only index to be classified as unreliable is ISR_0 .

24 **Table 8.** Average values (μ) and standard deviations (σ) of all healing indexes for the two mixtures,
 25 in the form $\mu \pm \sigma$. (CoV classes: **0-10%**, **10-20%**, **20-30%**, **30-40%**, **40-50%**, **>50%**)

month	mixture without crystalline admixture									
	chloride penetration				water permeability		flexural tests on thin beams			
	CPD [mm]/[%]	CPAcr [mm]/[%]	CPAun [mm]/[%]	ICS [-]/[%]	IPR [-]/[%]	ICS [-]/[%]	ISR ₀ [-]/[%]	ISR _{i-1} [-]/[%]	IRR [-]/[%]	ICS [-]/[%]
0	0	0	0	0	0	0	0	0	1	0
1	3.57/±37	7.45/±12	2.79/±75	0.37/±41	0.76/±21	0.38/±56	0.19/±149	0.19/±149	0.88/±8	0.62/±52
3	4.83/±17	13.26/±10	4.01/±29	0.82/±15	0.89/±8	0.56/±47	0.22/±55	1.04/±68	0.91/±43	0.62/±42
6	5.17/±20	13.74/±33	3.52/±21	0.76/±26	0.95/±6	0.67/±43	0.30/±123	1.12/±41	0.93/±24	0.61/±31
month	mixture with crystalline admixture									
	chloride penetration				water permeability		flexural tests on thin beams			
	CPD [mm]/[%]	CPAcr [mm]/[%]	CPAun [mm]/[%]	ICS [-]/[%]	IPR [-]/[%]	ICS [-]/[%]	ISR ₀ [-]/[%]	ISR _{i-1} [-]/[%]	IRR [-]/[%]	ICS [-]/[%]
0	0	0	0	0	0	0	0	0	1	0
1	3.73/±26	8.85/±41	3.56/±40	0.50/±45	0.71/±27	0.40/±55	0.41/±74	0.41/±74	0.89/±12	0.68/±48
3	3.57/±20	10.36/±18	3.73/±37	0.70/±34	0.85/±15	0.56/±44	0.23/±83	0.85/±40	0.89/±20	0.69/±54
6	3.87/±19	9.51/±75	2.68/±38	0.88/±18	0.90/±11	0.63/±44	0.16/±111	0.91/±33	1.01/±10	0.61/±57
eval.	medium	medium	medium	medium	high	low	insuff.	low	medium	low

1 **3.5. Considerations about statistical analyses within a standard-oriented framework**

2 The sizable amount of data related to crack-sealing allows for a statistical analysis aimed at possibly
3 shaping a standard-oriented approach for taking into account self-healing in the design of concrete
4 structures. In particular, while the datasets related to indexes CPD, CPA, IPR, ISR and IRR are limited
5 (since each specimen is associated to a single value), ICS in thin beams subjected to 4-Point Bending
6 is evaluated for several cracks for each specimen (since multiple cracking is observed in such case).
7 On the other hand, for chloride penetration tests and permeability tests on disks, one single value of
8 ICS is associated to each specimen, since in those tests pre-cracking was performed via splitting and
9 a single crack has been observed in the disks. For this reason, a statistical analysis has been performed
10 only on the ICS index related to thin beams, by assuming a Gaussian distribution of the results.

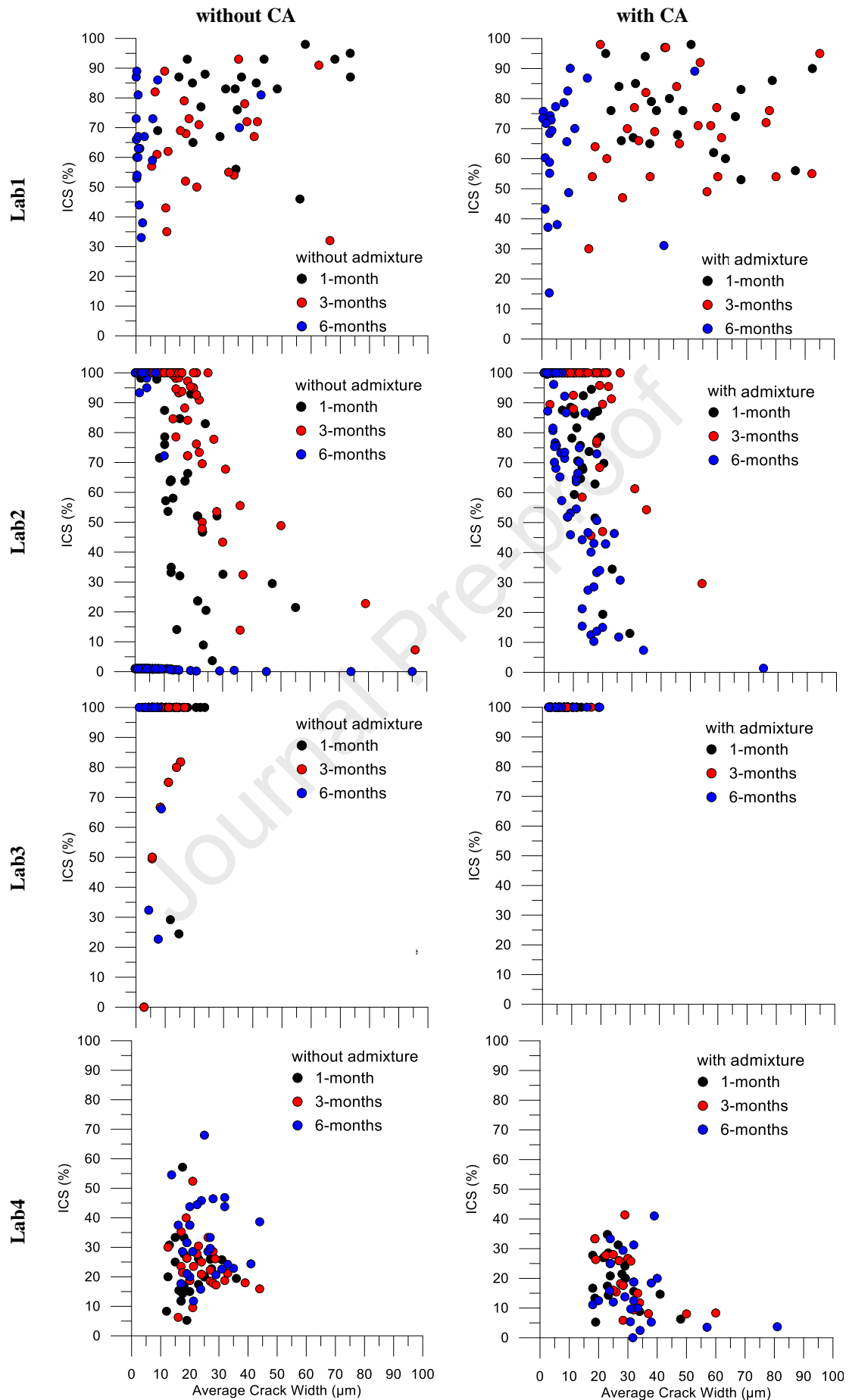
11 In Figure 14, the values of ICS for every crack observed in thin beams are shown, divided for partic-
12 ipating laboratory and for mixtures without and with crystalline admixture. First of all, it can be high-
13 lighted that a significant difference in terms of crack opening is observable among the laboratories,
14 even though the majority of cracks has a width smaller than 50 μm for all the partners.

15 Despite that for Lab1 cracks up to 100 μm can be observed, while no crack larger than 30 μm was
16 observed by Lab3, in the whole the crack ranges investigated by the different participants appear to
17 be quite consistent. However, a large scatter in the values of ICS has still been observed.

18 Lab3 shows the highest repeatability with very high values of ICS, mostly indicating perfect recovery
19 already after 1-month healing. On the opposite, Lab4 shows the lowest values of healing, with a good
20 consistency of the results, since most of the results are in the range 5-35%. Finally, Lab1 and Lab2
21 observed a sizably larger dispersion of data. As already highlighted in the previous section, however,
22 the final average values of ICS (averaged for each healing period) are rather in agreement among
23 Lab1, Lab2 and Lab3, while they are significantly lower in the case of Lab4 (see Figure 13).

24 In order to further investigate possible relationships between ICS and crack width, linear regression
25 algorithms have been applied to the presented dataset. Considering the results related to a single la-
26 boratory, a given healing duration (0-1 months, 1-3 months or 3-6 months) and one UHPFRCC mix-
27 ture, the x axis representing the crack width has been discretized in 10 μm -wide ranges. Within each
28 of them, all values of ICS associated to the crack-width falling in the range have been averaged, so
29 to define a unique value of ICS. For the same set, the standard variation has been estimated.

30 Triangular symbols in Figure 15 show averaged values of ICS observed at Lab1, differentiating for
31 the two mixtures and the three healing periods. In the same plot, the continuous line represents the
32 regression line associated to the average values. On the opposite, the dashed line represents the re-
33 gression curve of the characteristic values, where “characteristic values” refer to the 5th percentile,
34 namely the value of ICS which is overcome by 95 % of cracks with a width falling in the given range.



1

Figure 14. ICS for the mixtures without and with CA divided by laboratory and mixture

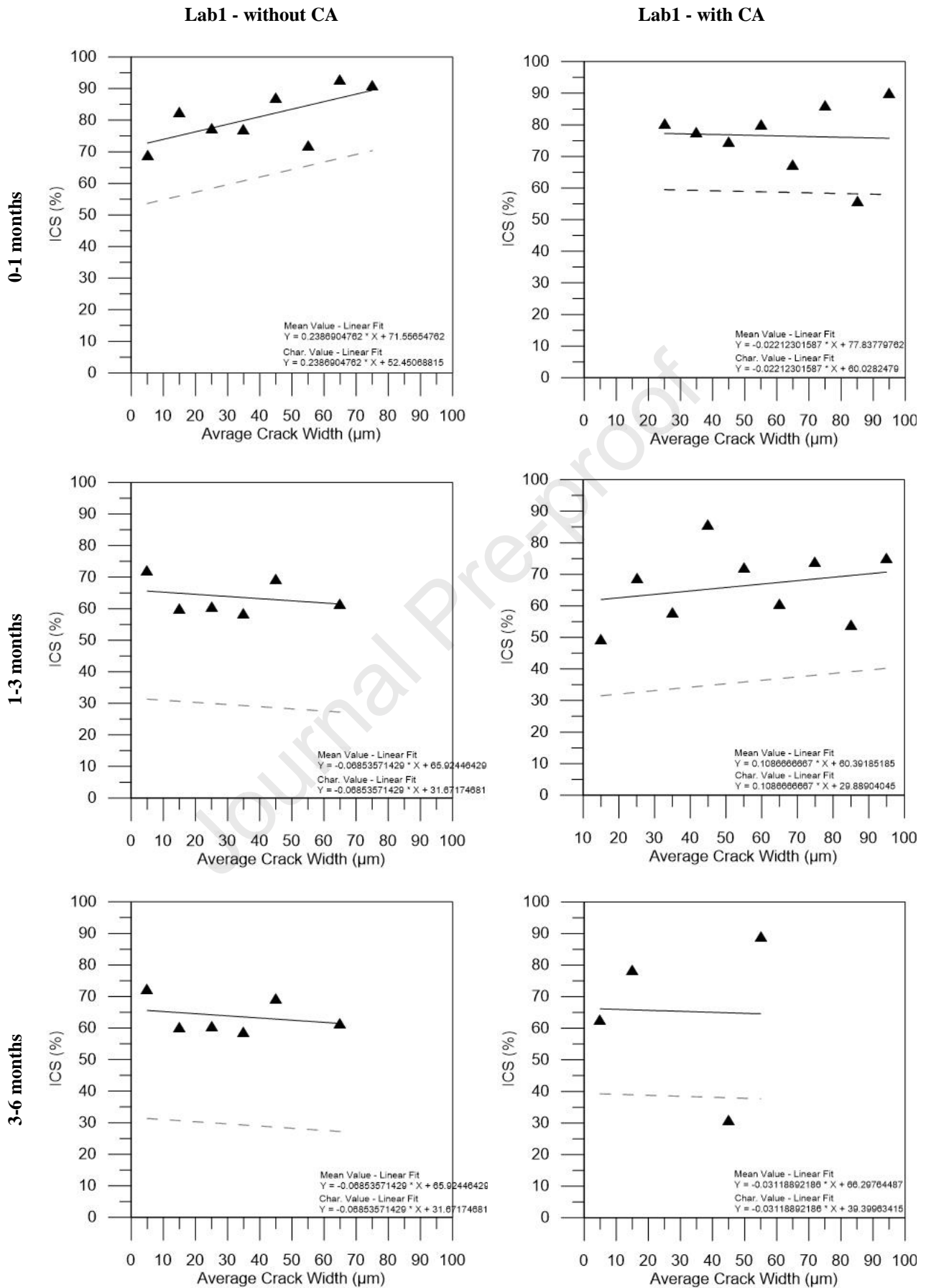
1 It is worth noting that average regression line and characteristic regression line are parallel since a
2 common standard deviation has been defined for all crack width ranges, calculated as a weighted
3 average among all standard deviations related to the different crack-width ranges. This has been car-
4 ried out differentiating for the two mixtures and for the three healing periods. Such approach has been
5 followed in order to define the characteristic values also in crack-width ranges in which the amount
6 of data was too limited for a good estimation of standard deviation. Characteristic values have been
7 evaluated assuming a Gaussian distribution of the data.

8 Regression lines allow to possibly highlight trends in the ICS with respect to the initial crack width.
9 Starting from the results by Lab1, it appears as ICS seems almost independent from the crack width.
10 On the contrary it could be expected that ICS decreases with the initial crack width due to the increased
11 difficulty in sealing larger cracks. It should be noted, however, that the overall range of crack width
12 herein studied is associated to very small cracks hardly larger than 80 μm , hence it can be considered
13 reasonable that the ICS is not significantly affected by initial crack width. Such outcome is confirmed
14 by Lab3 for very small cracks ($< 20\mu\text{m}$, see Figure 17), while a different trend has been observed in
15 Lab2 (Figure 16) and Lab4 (Figure 18).

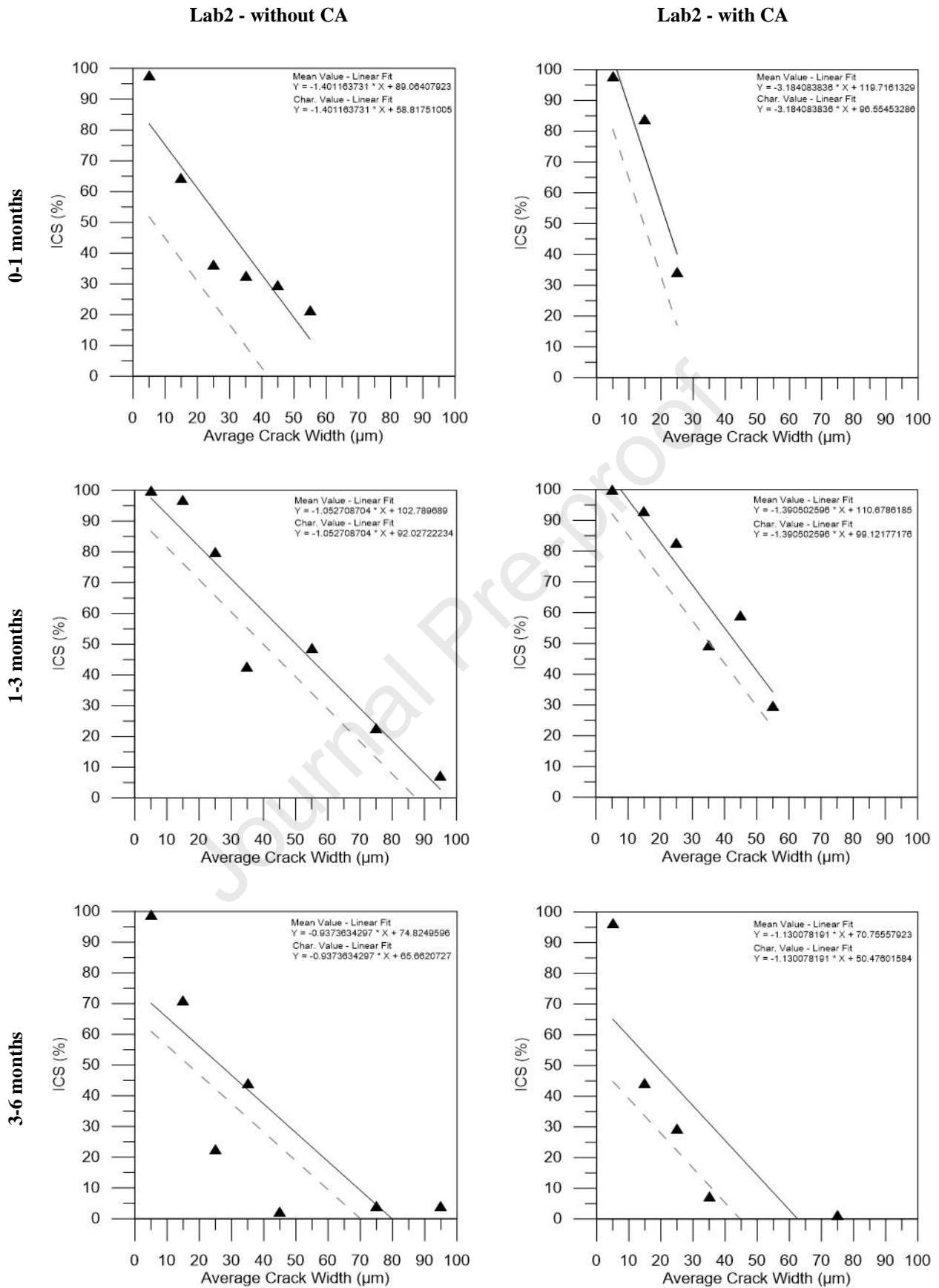
16 In particular, in Lab2, a strong dependence of ICS on initial crack width can be detected with clear
17 trends in the healing periods 0-1 months and 1-3 months and more scattered data in the period 3-
18 6 months. From the results, it can be stated that no crack sealing can be expected for a crack-width
19 larger than 100 μm even for long healing durations.

20 Finally, Figure 19 reports the regression lines obtained by considering the results of all participants
21 together. An intermediate trend between Lab1 and Lab2 can be observed, also because of the larger
22 dataset provided by these two laboratories. In Figure 19, however, a sizable scattering of data is noted
23 which decreases the reliability of the linear regression in matching the experimental data.

24 On the other hand, the linear regression represents an easy tool in taking into account crack *healability*,
25 meant as the capability of sealing a crack dependently on the initial crack width. Diagrams of *healability*
26 could be potentially used in the design at the Service Limit State (SLS) of structures made of UHPC,
27 with or without ordinary reinforcement. If a linear ICS versus crack-width behaviour is assumed, *heal-*
28 *ability* can be expressed by two parameters only. In Table 9, for example, the two parameters are chosen
29 to be the expected values of ICS for the two reference crack-widths of 30 and 50 μm . Table 9 highlights
30 that crystalline admixture (CA) leads to higher values of healing practically for all healing durations.
31 In some cases, Table 9 shows decreasing values of ICS with the healing time due to the repeated
32 cracking (previously referred to as *re-cracking*) performed at the beginning of each period (thus at 1
33 and 3 months) in small beams under bending. Repeated cracking lead to partially re-opening previ-
34 ously healed cracks in order to reproduce realistic structural cases subjected to variable loads.

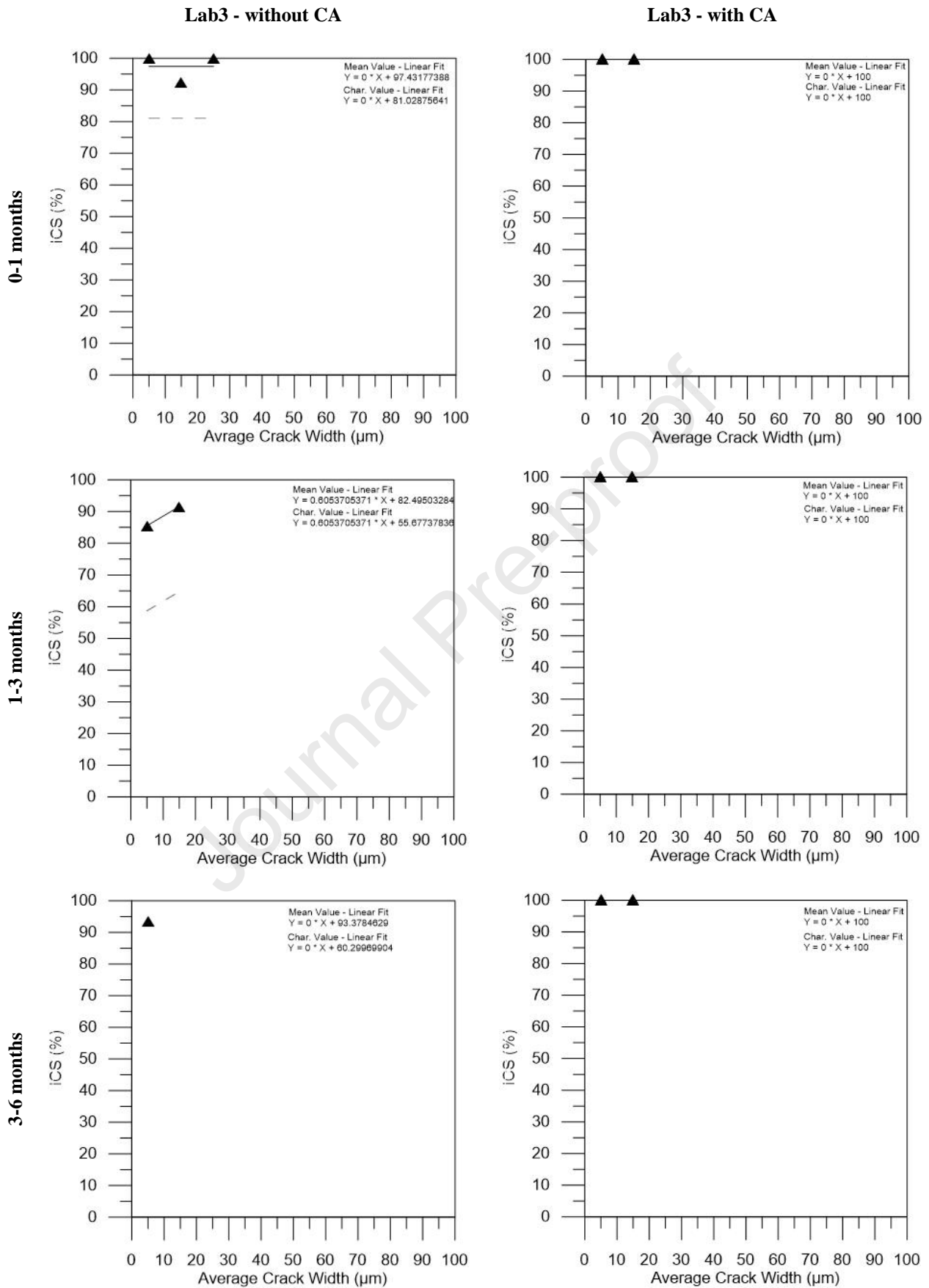


1 **Figure 15.** Lab1: Average values of ICS for the mixtures without and with CA for the different
 2 healing periods and regression lines associated to average and characteristic values



1

2 **Figure 16.** Lab2: Average values of ICS for the mixtures without and with CA for the different
 3 healing periods and regression lines associated to average and characteristic values

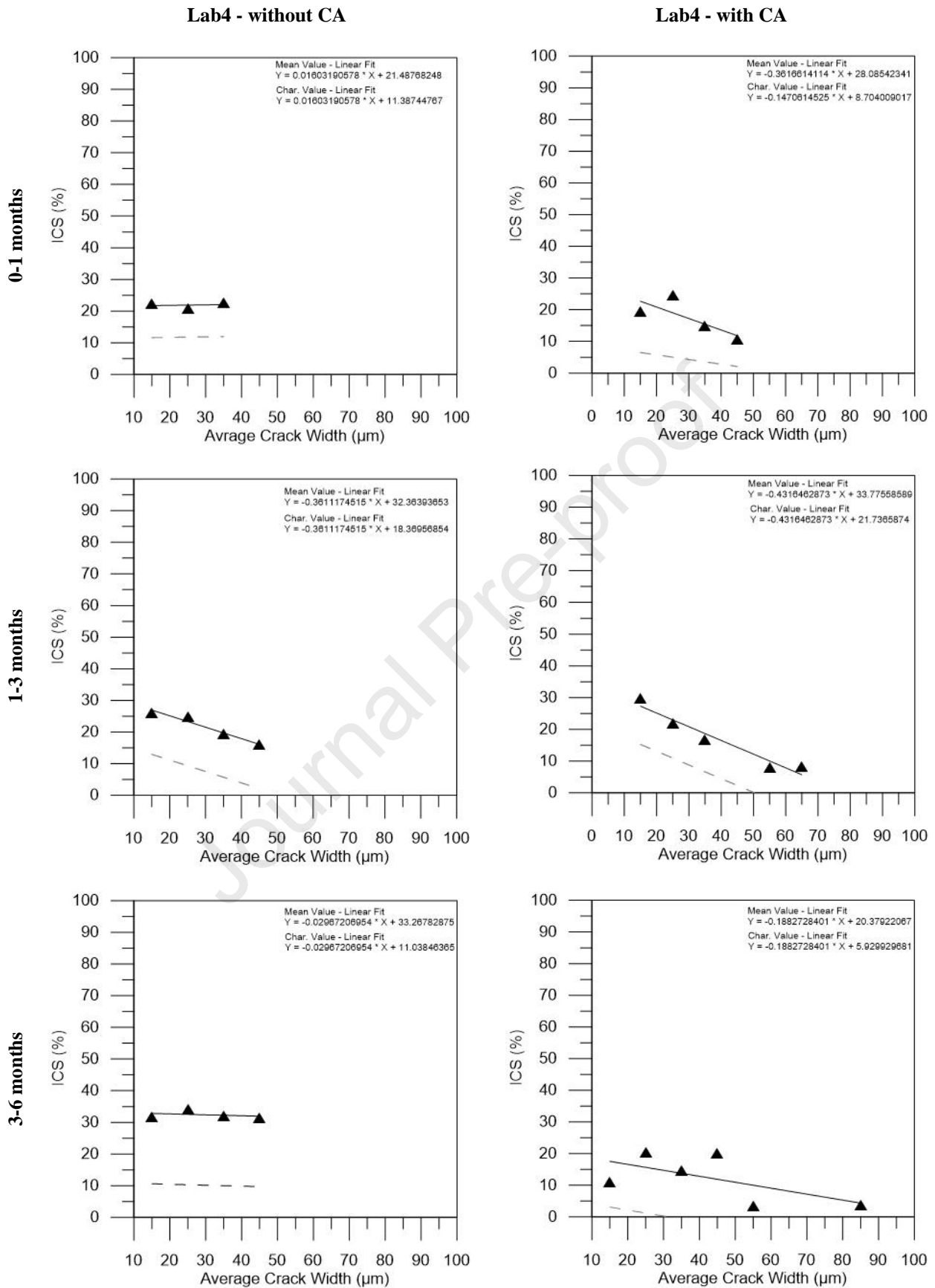


1

2

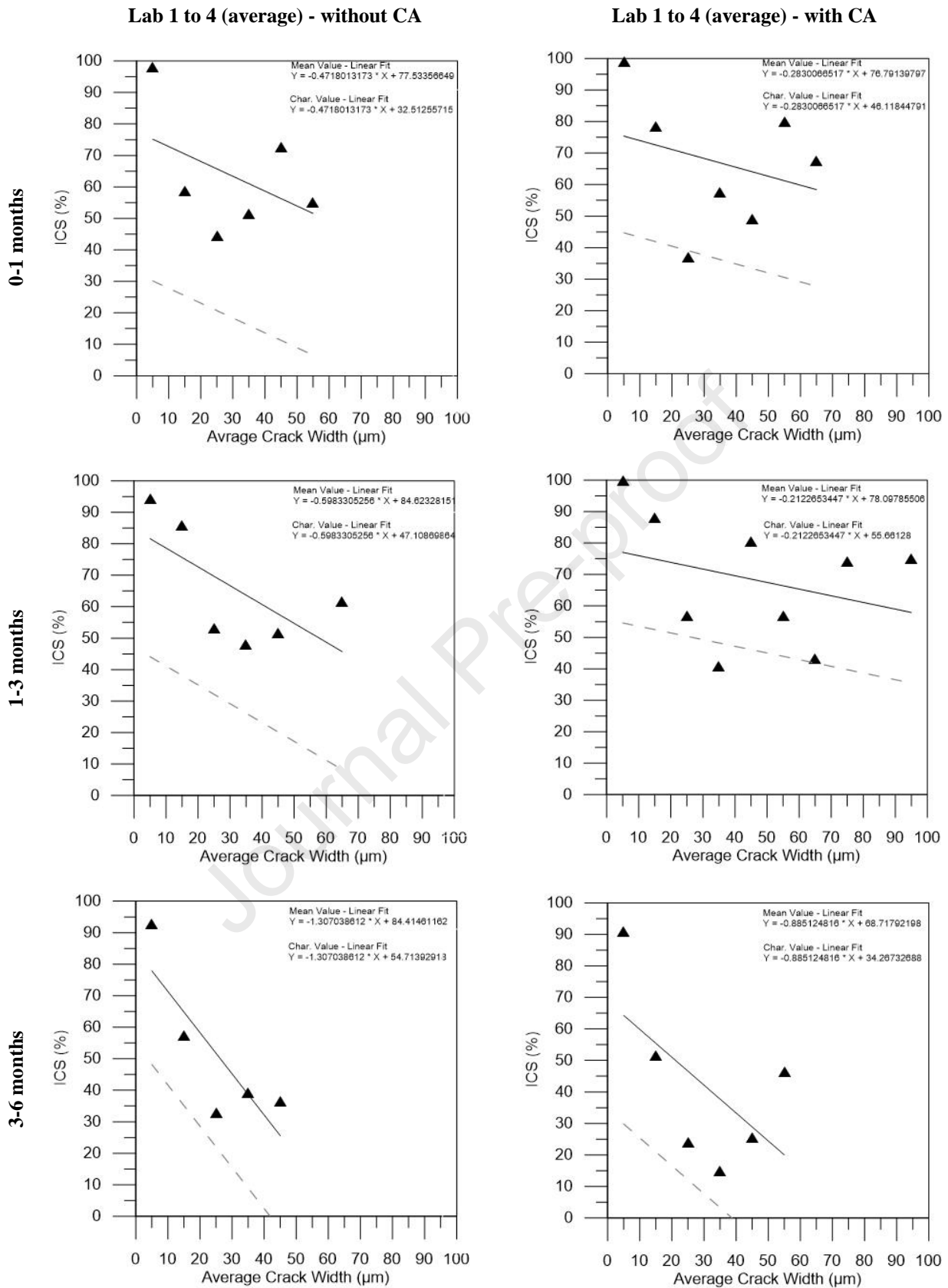
3

Figure 17. Lab3: Average values of ICS for the mixtures without and with CA for the different healing periods and regression lines associated to average and characteristic values



1

2 **Figure 18.** Lab4: Average values of ICS for the mixtures without and with CA for the different
 3 healing periods and regression lines associated to average and characteristic values



1

2

3

4

Figure 19. Lab1, Lab2, Lab3, Lab4: Average values of ICS for the mixtures without and with CA for the different healing periods and regression lines associated to average and characteristic values

Table 9. Expected average values of ICS at 30 and 50 μm , according to statistical analysis

crack width [mm]	0-1 months		1-3 months		3-6 months	
	W/O CA	With CA	W/O CA	With CA	W/O CA	With CA
30 μm	0.63	0.68	0.67	0.72	0.45	0.42
50 μm	0.54	0.63	0.55	0.67	0.19	0.25

4. CONCLUSIONS

The present paper has reported the main results yielded by the inter-laboratory test campaign performed on Ultra High-Performance Fibre-Reinforced Cementitious Composites (UHPFRCCs) organized under the umbrella of the COST Action CA15202 SARCOS (Self-healing As prevention Repair of COncrete Structures). The major objective of the campaign was to discuss, in terms of repeatability and consistency, a multi-performance methodology for self-healing assessment in UHPFRCCs.

The multi-performance approach has been conceived so to thoroughly investigate the effect of self-healing on both durability and mechanical responses of concrete and concrete structures, having in mind possible real applications of UHPFRCCs.

The experimental procedure is based on three test setups, mostly based on quite established experimental procedures adopted in the research community active on the topic. In particular, the three tests herein implemented are: (1) chloride penetration test on pre-cracked disks, (2) water permeability test on pre-cracked disks and (3) repeated 4-point flexural test on thin beams. The first test is meant to provide information related to the penetration rate of chloride, the second one to investigate the ability of cracks to recover water-tightness thanks to crack-sealing, while the third one aims at assessing the mechanical performance recovery in terms of strength and stiffness. This latter entails not only the capability of sealing cracks, but also the ability to maintain them closed under applied tension, thanks to crack filling and fibre-matrix bond improvement.

Two UHPFRCC mixtures have been studied, both containing 1.5% by volume of steel fibres, while just in one of the two a crystalline admixture has been added as a healing promoter. Self-healing has been quantified through a set of suitably defined indices which also allowed a cross-comparison of results among different tests.

On the base of the data collected from all the laboratories involved and their comparison, the following conclusions can be drawn:

- The test on water permeability is the one showing the highest repeatability, even more when considering that 6 of the 7 working groups performed this test. A rather rapid and efficient recovery of water tightness has been observed already after one month of healing. Despite of the overall repeatability of the results, the differences between the average curves related to the two mixes is comparable with data scattering, thus not allowing to clearly highlight the role played by crystalline admixture.

- 1 • The indices linked to chloride penetration (measured via silver nitrate) also proved a good agree-
2 ment among the laboratories, even though just three working groups participated to this task.
3 Among the three parameters, Crack Penetration Depth – CPD, Crack Penetration Average depth –
4 CPA on un-cracked disks and CPA on cracked disks, the first and the second ones proved to be
5 analogous. The former resulted to be more consistent and repeatable than the second, thus sug-
6 gesting that CPA on un-cracked disks could be removed from a possible panel of main healing-
7 related parameters.
- 8 • Regarding the healing-related mechanical indices, the one related to resistance recovery (IRR)
9 resulted to be the most robust one. Far larger scattering was observed for the indexes linked to
10 stiffness, this being probably due to its more complex evaluation with respect to the others.
- 11 • Despite its apparent simplicity, the index of surface-crack healing or crack sealing (ICS), based on
12 visual inspection of cracks surface before and after healing, showed a sizable scattering among the
13 laboratories. This can be partly attributed to differences in the initial crack opening. However, this
14 is still under scrutiny, since such parameter is one of the most widely used in the research commu-
15 nity for assessing self-healing extent on cementitious materials.
- 16 • Focusing on the behaviour of the two UHPFRCCs and the potential positive role of the crystalline
17 admixture as a stimulator of autogenous healing, the scattering of the results related to different
18 laboratories made it difficult to clearly highlight its benefits. Despite that, a faster and less scattered
19 healing was observed in some cases, irrespective of the test and of the testing laboratory. This
20 outcome can be also attributed to the fact that, thanks to the presence of a significant amount of
21 anhydrous particles and the very narrow cracks generated by multiple cracking, autogenous heal-
22 ing in UHPFRCC is particular efficient. This smooths down the beneficial role played by crystal-
23 line admixture in self-healing processes. Such aspect, together with the mentioned scattering
24 among laboratories' data, did not allow to properly assess a difference between the two mixtures.
- 25 • According to the discussion about data consistency as reported in Section 3.4, all the indices ap-
26 pear to be satisfactorily consistent, except for the index of stiffness recovery, whose variation
27 among laboratories resulted to be excessively high.
- 28 • A statistical analysis was performed on the widest dataset which was related to the index of crack-
29 sealing (ICS) in thin beams (since multiple cracking in such specimens enabled the evaluation of
30 dozens of values for each laboratory). The significance of the concept of “*crack-width healability*”
31 coming from the correlation of self-healing recovery and initial crack width was highlighted. Such
32 view is expected to push self-healing concepts within a design-oriented framework even though
33 further efforts should be made to increase the overall confidence of the approach.
- 34 The preliminary statistical analysis of the data, together with the concept of “*crack-width healability*”,

1 can be considered as a first step in the direction of incorporating self-healing concepts into code-
 2 based design approaches. This includes a future perspective of systematically implementing defined
 3 meta-analysis algorithms, which, by managing and processing significant amounts of data from the
 4 available literature, will also allow to provide confidence ranges for the proposed correlations.
 5 It is worth noting that, despite a multi-performance approach should be preferred for the assessment
 6 of self-healing capability in UHPFRCCs (according to the specific structural application), for initial
 7 material screening a single reference test could be adopted. For the sake of simplicity, the index of
 8 crack sealing measured on cracked disks appears to be the most suitable. On the other hand, for a
 9 comprehensive characterization of the materials towards typical structural applications, flexural test-
 10 ing (even in combination with chloride penetration on disks) appears to be the most meaningful.
 11 Finally, water permeability test can be considered for hydraulic applications as basins, ducts or con-
 12 taining walls/linings under the water table.

13 **ACKNOWLEDGMENTS**

14 The round robin activity reported in this paper has been performed in the framework of the COST
 15 Action CA 15202 “SARCOS” (Self-healing As prevention Repair of COncrete Structures,
 16 <http://www.sarcos.eng.cam.ac.uk>). The production of the material and the inter-laboratory compari-
 17 son were also supported by the ReSHEALience project (Rethinking coastal defence and Green-en-
 18 ergy Service infrastructures through enHancEd-durAbiLity high-performance cement-based materi-
 19 als) which has received funding from the European Union’s Horizon 2020 research and innovation
 20 program under grant agreement No 760824 (www.uhdc.eu).

21 **REFERENCES**

- 22 [1] HEALCON. Self-healing concrete to create durable and sustainable concrete structures. University of Gent,
 23 Grant Agreement ID 309451; 2013.
- 24 [2] M4L. Materials for life (M4L): biomimetic multi-scale damage immunity for construction materials, Cardiff
 25 University. EPSRC (Engineering and Physical Sciences Research Council). EP/K026631/ 1; 2013.
- 26 [3] CAPDESIGN. Encapsulation of polymeric healing agents in self-healing concrete: capsule design. De Belie
 27 Nele, 2014.
- 28 [4] LORCENIS. LOng Lasting Reinforced Concrete for ENergy Infrastructure under severe operating conditions.
 29 European Union’s Framework Programme for Research and Innovation Programme under Grant Agreement
 30 No 685445; 2016.
- 31 [5] Action CA15202 — Self-Healing as Preventive Repair of COncrete Structures. 2016–2021, European Coop-
 32 eration in Science and Technology (COST). Available online: [https://www.cost.eu/ac-](https://www.cost.eu/actions/CA15202/#tabs|Name:overview)
 33 [tions/CA15202/#tabs|Name:overview](https://www.cost.eu/actions/CA15202/#tabs|Name:overview) (accessed on 24 February 2021). www.sarcos.eng.cam.ac.uk/

- 1 [6] RM4L. Resilient Materials 4 Life (RM4L), Cardiff University. EPSRC – Engineering and Physical Sciences
2 Research Council; 2017.
- 3 [7] EndurCrete. New environmental friendly and durable concrete. European Union’s Framework Programme for
4 Research and Innovation Programme, Grant Agreement. No 760639; 2018.
- 5 [8] ReSHEALience. European Union’s Framework Programme for Research and Innovation Programme under
6 Grant Agreement No 760824; 2018. www.uhdc.eu.
- 7 [9] SMARTINCS, Self-Healing – Multifunctional – Advanced Repair Technologies in Cementitious Systems,
8 European Union’s Framework Programme for Research and Innovation Programme under Marie Skłodowska-
9 Curie Grant Agreement SMARTINCS No 860006 Priv. Policy; 2019. Available from:
10 <https://smartincs.ugent.be/index.php/about-us>.
- 11 [10] Cappellesso V., di Summa D., Pourhaji P., Prabhu Kannikachalam N., Dabral K., Ferrara L., Cruz Alonso M.,
12 Camacho E., Gruyaert E., De Belie N. (2023) “A review of the efficiency of self-healing concrete technologies
13 for durable and sustainable concrete under realistic conditions”, *International Materials Reviews*
- 14 [11] Dry C. M. (1999) “Repair and prevention of damage due to transverse shrinkage cracks in bridge decks”. *Smart*
15 *Struct Mater.* 3671, pp. 253–256. doi: 10.1117/12. 348675.
- 16 [12] Davies R, Teall O, Pilegis M, et al. (2018) “Large scale application of self-healing concrete: design, construc-
17 tion, and testing”. *Front Mater.* 5:1–12. doi:10.3389/fmats.2018.00051.
- 18 [13] Sierra-Beltran M. G., Jonkers H. M., Ortiz M. (2015) “Field application of self-healing concrete with natural
19 fibres as linings for irrigation canals in Ecuador”. *Fifth International Conference on Self-Healing Materials;*
20 *Durham, NC. Vol. 32, pp. 1–4.*
- 21 [14] Van Tittelboom K., Wang J., Araújo M., et al. (2016) “Comparison of different approaches for self-healing
22 concrete in a large-scale lab test”. *Constr Build Mater.* 107, pp.125–137.
- 23 [15] Al-Tabbaa A., Litina C., Giannaros P., et al. (2019) “First UK field application and performance of microcap-
24 sule-based self-healing concrete”. *Constr Build Mater.* 208:669–685. doi: 10.1016/j.conbuildmat.2019.
25 02.178.
- 26 [16] Selvarajoo T, Davies RE, Gardner DR, et al. Characterisation of a vascular self-healing cementitious material
27 system: flow and curing properties. *Constr Build Mater.* 2020;245:118332. doi:10.1016/j.
28 conbuildmat.2020.118332.
- 29 [17] Selvarajoo T, Davies R, Freeman B, et al. Mechanical response of a vascular self-healing cementitious material
30 system under varying loading conditions. *Constr Build Mater.* 2020;254:119245. doi:10.1016/j.
31 conbuildmat.2020.119245.
- 32 [18] Van Mullem T, Gruyaert E, Caspeepe R, et al. First large scale application with self-healing concrete in Bel-
33 gium: analysis of the laboratory control tests. *Materials.* 2020;13:997. doi:10.3390/ma13040997.
- 34 [19] Al-Obaidi S., Davolio M., Lo Monte F., Costanzi F., Luchini M., Bamonte P. and Ferrara L., (2022), “Struc-
35 tural Validation of Geothermal Water Basins constructed with Durability Enhanced Ultra High-Performance
36 Fiber Reinforced Concrete”, *Case Studies in Construction Materials*, 17, art. no. e01202.
- 37 [20] Tenório Filho, J.R., Mannekens, E., Van Tittelboom, K., Van Vlierberghe, S., De Belie, N. and Snoeck, D.

- 1 (2021). Innovative SuperAbsorbent Polymers (iSAPs) to construct crack-free reinforced concrete walls: an
2 in-field large-scale testing campaign, *Journal of Building Engineering*, 102639, 1-12.
- 3 [21] Cuenca, E., Postolachi, V., Ferrara, L. (2023) “Cellulose nanofibers to improve the mechanical and durability
4 performance of self-healing ultra-high performance concretes exposed to aggressive waters”. *Constr Build
5 Mater.* 374, 130785. Doi: 10.1016/j.conbuildmat.2023.130785.
- 6 [22] Xi, B., Al-Obaidi, S., Ferrara, L. (2023) “Effect of different environments on the self-healing performance of
7 ultra high-performance concrete – A systematic literature review”. *Constr Build Mater.* 374, 130946. Doi:
8 10.1016/j.conbuildmat.2023.130946.
- 9 [23] Davolio, M., Al-Obaidi, S., Altomare, Y., Lo Monte, F. and Ferrara, L., (2023), “A methodology to assess the
10 evolution of mechanical performance of UHPC as affected by autogenous healing under sustained loadings
11 and aggressive exposure conditions”. *Cem Concr Compos.* 139, 105058. Doi: 10.1016/j.cemcon-
12 comp.2023.105058.
- 13 [24] XI, B., Huang, Z., Al-Obaidi, S. and Ferrara, L. “Predicting High-Performance Concrete (UHPC) self-healing
14 performance using hybrid models based on metaheuristic optimization techniques”. *Constr Build Mater.* Re-
15 submitted for re-reviews February 2nd, 2023.
- 16 [25] Kannikachalam, N.P., di Summa, D., Borg, R.P., Cuenca, E., Parpanesi, M., De Belie, N. and Ferrara, L.:
17 “Assessment of Sustainability and self-healing performances of recycled ultra-high-performance concrete”.
18 *ACI Journal.* 120(1), pp. 117-132. <https://dx.doi.org/10.14359/51737336>.
- 19 [26] Zabalza Bribián I., Capilla A. V., Aranda Usón A. (2011) “Life cycle assessment of building materials: Com-
20 parative analysis of energy and environmental impacts and evaluation of the eco-efficiency improvement po-
21 tential”. *Build Environ.* 46(5), pp. 1133-1140.
- 22 [27] Banthia, N. (2008) “Fiber reinforced concrete for sustainable and intelligent infrastructure.” *Proc. of First Int.*
23 *Conf. on Microstructure Related Durability of Cementitious Composites.* Rilem, Nanjing.
- 24 [28] J. R Mackechnie, M. G Alexander, (2009), “Using Durability to Enhance Concrete Sustainability”, *Journal of*
25 *Green Building* 4 (3): 52–60. <https://doi.org/10.3992/jgb.4.3.52>
- 26 [29] Van den Heede P, Mignon A, Habert G, et al. (2018) Cradle-to-gate life cycle assessment of self-healing engin-
27 eered cementitious composite with in-house devel-oped (semi-)synthetic superabsorbent polymers. *Cem*
28 *Concr Compos.* 94, pp.166–180.
- 29 [30] Van den Heede P, De Belie N, Pittau F, et al. Life cycle assessment of self-healing engineered cementi-
30 tious composite (SH-ECC) used for the rehabilitation of bridges. *Life Cycle Analysis and Assessment in Civil En-*
31 *gineering: Towards an Integrated Vision Proceedings of the Sixth Inter. Symposium on Life-Cycle Civil En-*
32 *gineering, IALCCE 2018, 2019.* p. 2269–2275.
- 33 [31] Huang, L.; Krigsvoll, G.; Johansen, F.; Liu, Y.; Zhang, X. Carbon emission of global construction sector.
34 *Renew. Sustain. Energy Rev.* 2018, 81, 1906–1916.
- 35 [32] Ferrara, L., Van Mullem, T., Alonso, M.C., Antonaci, P., Borg, R.P., Cuenca, E., Jefferson, A., Ng, P.L., Peled,
36 A., Roig, M., Sanchez, M., Schroefl, C., Serna, P., Snoeck D., Tulliani, J.M. and De Belie, N.: “Experimental

- 1 characterization of the self-healing capacity of cement based materials and its effects on the material perfor-
2 mance: a state of the art report by COST Action SARCOS WG2”, *Construction and Building Materials*, 167,
3 10 April 2018, pp. 115-142.
- 4 [33] De Belie, N., Gruyaert, E., Al-Tabbaa, A., Antonaci, P., Baera, C., Bajare, D., Darquennes, A., Davies, R.,
5 Ferrara, L., Jefferson, T., Litina, C., Miljevic, B., Otlewska, A., Ranogajec, J., Roig-Flores, M., Pain, K., Lu-
6 kowski, P., Serna, P. Tulliani, J.M., Vucetic, S., Wang, J., Jonkers, H.M.: “A review of self-healing concrete
7 for damage management of structures”, *Advanced Materials and Interfaces*, vol 5, issue 17, September 2018,
8 pp. 1-28. DOI: 10.1002/admi.201800074.
- 9 [34] Jefferson, T., Javierre, E., Lee Freeman, B., Zaoui, A., Koenders, E. and Ferrara, L.: “Research progress on
10 numerical models for self-healing cementitious materials”, *Advanced Materials and Interfaces*, volume 5, issue
11 17, September 2018, pp. 1-19. DOI: 10.1002/admi.201701378
- 12 [35] Al-Obaidi, S., Bamonte, P., Luchini, M., Mazzantini, I. and Ferrara, L.: “Durability-based design of structures
13 made with UHP/UHDC in extremely aggressive scenarios: application to a geothermal water basin case
14 study”, *MDPI Infrastructures*, 5 (11), November 2020, pp. 1-44, [http://dx.doi.org/10.3390/infrastruc-](http://dx.doi.org/10.3390/infrastructures5110102)
15 [tures5110102](http://dx.doi.org/10.3390/infrastructures5110102).
- 16 [36] Escoffres, P., Desmettre, C. and Charron, J.P., “Effect of crystalline admixtures on the self-healing capability
17 of high performance fiber reinforced concretes in service conditions”, *Construction and Building Materials*,
18 vol. 173, pp. 763–774, 2018.
- 19 [37] di Summa, D., Tenorio Filho, J.R., Snoeck, D., Van den Heede, P., Van Vierberghe, S., Ferrara, L. and De
20 Belie, N.: “Environmental and economic sustainability of crack mitigation in reinforced concrete with Super-
21 Absorbent Polymers (SAPs)”, *Journal of Cleaner Production*, vol 58, July 2022, pp. 1-15,
22 <https://doi.org/10.1016/j.jclepro.2022.131998>.
- 23 [38] M. Maes, K. Van Tittelboom and N. De Belie, "The efficiency of self-healing cementitious materials by means
24 of encapsulated polyurethane in chloride containing environments", *Construction and Building Materials*, vol.
25 71, pp. 528-537, 2014.
- 26 [39] B. Savija and E. Schlangen, "Autogeneous healing and chloride ingress in cracked concrete," *HERON*, vol.
27 61, no. 1, pp. 15-32, 2016.
- 28 [40] M. Sahmaran, "Effect of flexure induced transverse crack and self-healing on chloride diffusivity of reinforced
29 mortar," *Journal of Material Science*, vol. 43, pp. 9131-9136, 2007
- 30 [41] S. Jacobsen and E. Sellevold, "Self-healing of high strength concrete after deterioration by freeze/thaw," *Ce-*
31 *ment and Concrete Research*, vol. 26, pp. 55-62, 1995.
- 32 [42] M. Ismail and e. al, "Effect of crack opening on the local diffusion of chloride in cracked mortar sample,"
33 *Cement and Concrete Research*, vol. 38, pp. 1106-1111, 2008.
- 34 [43] R. Borg, E. Cuenca, E. GastaldoBrac and L. Ferrara, "Crack sealing capacity in chloride-rich environments of
35 mortars containing different cement substitutes and crystalline admixtures," *Journal of Sustainable Cement-*
36 *Based Materials*, vol. 7, no. 3, pp. 141-159, 2018.
- 37 [44] Cuenca, E., Rigamonti, S., Gastaldo Brac, E. and Ferrara, L.: “Improving resistance of cracked concrete to

- 1 chloride diffusion through “healing stimulating” crystalline admixtures”, *ASCE Journal of Materials in Civil*
 2 *Engineering*, vol. 33 (3), March 2021, paper 04020491, pp- 1-14, [https://doi.org/10.1061/\(ASCE\)MT.1943-](https://doi.org/10.1061/(ASCE)MT.1943-)
 3 5533.0003604
- 4 [45] H. Ling and Q. Chunxiang, (2017) "Effects of self-healing cracks in bacterial concrete on the transmission of
 5 chloride during electromigration," *Constr. and Build. Mat.* 144, pp. 406-411.
- 6 [46] B. Van Belleghem, P. Van den Heede, K. Van Tittelboom and e. al, "Quantification of the service life extension
 7 and environmental benefit of chloride exposed self-healing concrete," *Materials* 10 (5), pp. 1-22, 2017.
- 8 [47] Maes, M., Snoeck, D. and De Belie, N. (2016), “Chloride penetration in cracked mortar and the influence of
 9 autogenous crack healing”, *Construction and Building Materials*, 115, 114-124.
- 10 [48] Cuenca E., Lo Monte F., Moro M., Schiona A., Ferrara L. (2021), “Effects of autogenous and stimulated self-
 11 healing on durability and mechanical performance of UHPFRC: Validation of tailored test method through
 12 multi-performance healing-induced recovery indices”, *Sustainability (Switzerland)*, 13 (20), art. no. 11386.
- 13 [49] Cuenca E, Criado M, GimenezM, AlonsoMC, Ferrara L (2022) Durability of ultra-high performance fiber
 14 reinforced cementitious composites exposed to chemically aggressive environments: up-grading to ultra-high
 15 durability concrete through nano-constituents. *ASCE J Mater Civ Eng* 34(8), art. no. 04022154.
- 16 [50] Li, V.C. and Wu, H.C., 'Conditions for pseudo strain-hardening in fiber reinforced brittle matrix composites',
 17 *Appl. Mech. Rev.*, 45 (8) (1992) 390-398.
- 18 [51] Li, V.C., Stang, H. and Krenchel, H., 'Micromechanics of crack bridging in fibre-reinforced concrete', *Mats.*
 19 *& Struct.*, 26 (8) (1993) 486-494.
- 20 [52] Li, V.C., 'On engineered cementitious composites. A review of the material and its applications' *J. Adv. Concr.*
 21 *Tech.*, 1 (3) (2003) 215-230.
- 22 [53] da Cunha Moreira, T.N., Krelani, V., Ferreira, S.R., Ferrara, L. and Toledo Filho, R.D: “Self-healing of slag
 23 cement Ultra High Performance Steel Finer Reinforced Concrete (UHPFRC) containing sisal fibers as healing
 24 conveyor”, *Journal of Building Engineering*, vol 54, August 2022, paper 104638,
 25 <https://doi.org/10.1016/j.jobe.2022.104638>
- 26 [54] Lo Monte, F. and Ferrara, L.: “Tensile Behaviour Identification in Ultra-High Performance Fibre Reinforced
 27 Cementitious Composites: Indirect Tension Tests and Back Analysis of Flexural Test Results”, *Materials and*
 28 *Structures*, 2020, 53:145, pp. 1-12.
- 29 [55] Al Obaidi S., Bamonte P., Animato F., Lo Monte F., Mazzantini I., Luchini M., Sculari S., Ferrara L., (2021),
 30 "Innovative design concept of cooling water tanks/basins in geothermal power plants using ultra-high-perfor-
 31 mance fiber-reinforced concrete with enhanced durability", *Sustainability*, 13 (17), art. no. 9826.
- 32 [56] Qiu, J., He, S., Wang, Q., Su, H. and Yang, E.H.: “Autogenous healing of fibre/matrix interface and its en-
 33 hancement”, in *Proceedings Framcos X*, G. Pijaudier-Cabot et al., eds., 2019.
- 34 [57] Lo Monte, F. and Ferrara, L.: “Self-Healing Characterization of UHPFRCC with Crystalline Admixture: Ex-
 35 perimental Assessment via Multi-Test/Multi-Parameter Approach”, *Construction and Building Materials*, vol.
 36 33, May 2021, paper 122579, pp. 1-12, <https://doi.org/10.1016/j.conbuildmat.2021.122579>.
- 37 [58] Nele De Belie, Kim Van Tittelboom, Mercedes Sánchez Moreno, Liberato Ferrara and Elke Gruyaert, “Self-

- 1 healing concrete research in the European projects SARCOS and SMARTINCS”, in Proc. of the 3rd RILEM
2 Spring Convention and Conference (RSCC 2020).
- 3 [59] Litina C, Bumanis G, Anglani G, Dudek M, Maddalena R, Amenta M, Papaioannou S, Pérez G, García Calvo
4 JL, Asensio E, Beltrán Cobos R, Tavares Pinto F, Augonis A, Davies R, Guerrero A, Sánchez Moreno M,
5 Stryzewska T, Karatasios I, Tulliani JM, Antonaci P, Bajare D, Al-Tabbaa A. (2021) Evaluation of Method-
6 ologies for Assessing Self-Healing Performance of Concrete with Mineral Expansive Agents: An Interlabora-
7 tory Study. *Materials* 2021, 14, 2024, <https://doi.org/10.3390/ma14082024>.
- 8 [60] Marta Roig Flores, Hesam Doostkami, Maria Cruz Alonso, Lina Ammar, Diana Bajare, Rubén Beltrán Cobos,
9 Ruben Paul Borg, Girts Bumanis, Aveline Darquennes, Mercedes Gimenez, Rawan Hammoud, Henk M.
10 Jonkers, Ioannis Karatasios, Albany Milena Lozano Násner, Stamatoula Papaioannou, Michaela Reichardt,
11 Pavel Reiterman, Bettencourt Ribeiro, Claudia Romero Rodriguez, Mercedes Sánchez Moreno, Karyne San-
12 tos, Christof Schroefl and Pedro Serna, “Evaluation of the self-healing efficiency of concrete with a crystalline
13 admixture: Interlaboratory analysis from COST Sarcos RRT3 group”, in Proceedings of 8th International Con-
14 ference on Self-Healing Materials ICSHM-MILANO 2022.
- 15 [61] Van Mullem T, Anglani G, Dudek M, Vanoutrive H, Bumanis G, Litina C, Kwiecień A, Al-Tabbaa A, Bajare
16 D, Stryzewska T, Caspele R, Van Tittelboom K, Jean-Marc T, Gruyaert E, Antonaci P, De Belie N, (2020),
17 “Addressing the need for standardization of test methods for self-healing concrete: an inter-laboratory study
18 on concrete with macrocapsules”, *Science and Technology of Advanced Materials* 21 (1), pp.661-682.
- 19 [62] Chacra Sofia, “Avaliação da capacidade de autorregeneração de um biobetão”, Master Thesis 2022,
20 Universidade Nova de Lisboa (Supervisor: Faria Paulina). Jonkers, H. M. & Romero-Rodriguez, C. (2020).
21 RRT6 Concrete with Bacterial Admixtures - SARCOS – Interlaboratory Testing. Delft University of Technol-
22 ogy.
- 23 [63] Ferrara, L., Krelani, V. and Carsana, M: “A fracture testing based approach to assess crack healing of concrete
24 with and without crystalline admixtures”, *Construction and Building Materials*, 68, 2014, pp. 515-531.
- 25 [64] Ferrara, L., Krelani, V. and Moretti, F.: “On the use of crystalline admixtures in cement based construction
26 materials: from porosity reducers to promoters of self-healing”, *Smart Materials and Structures*, 25 (2016)
27 084002 (17pp) doi:10.1088/0964-1726/25/8/084002.
- 28 [65] Cuenca, E., Tejedor, A. and Ferrara, L.: “A methodology to assess crack sealing effectiveness of crystalline
29 admixtures under repeated cracking-healing cycles”, *Construction and Building Materials* 179, pp. 619-632.
- 30 [66] Cuenca, E., D’Ambrosio, L., Lizunov, D., Tretjakov, A., Volobujeva, O. and Ferrara, L.: “Mechanical prop-
31 erties and self-healing capacity of Ultra High Performance Fibre Reinforced Concrete with alumina nanofibers:
32 tailoring Ultra High Durability Concrete for aggressive exposure scenarios”, *Cement and Concrete Compo-
33 sites*, April 2021, paper 103956, 17 pp. <https://doi.org/10.1016/j.cemconcomp.2021.103956>.
- 34 [67] De Souza Oliverira, A. da Fonseca Martins Gomez, O., Ferrara, L., de Moraes Rego Fairbairn, E., Toledo
35 Filho, R.D., An Overview of a Twofold Effect of Crystalline Admixtures: from Permeability-Reducers to Self-
36 Healing Stimulators, *Journal of Building Engineering*, vol. 41, September 2021, paper 102400, pp. 1-20,
37 <https://doi.org/10.1016/j.jobbe.2021.102400>.

- 1 [68] Lo Monte F., Mezquida-Alcaraz E.J., Navarro-Gregori J., Serna P. and Ferrara L., “Mechanical Characteriza-
2 tion in Tension of UHPFRCs with Steel or Amorphous Metallic Fibres via a Combined Experimental/Numer-
3 ical Identification Procedure”, submitted to Structural Concrete (2023).
- 4 [69] Roig-Flores M., Moscato S., Serna. P. and Ferrara L., (2015) “Self-healing capability of concrete with crystal-
5 line admixtures in different environments”, *Contr. and Build. Mat.* 86, pp. 1-11.
- 6 [70] Roig Flores, M., Pirritano, F., Serna Ros, P. and Ferrara, L.: “Effect of crystalline admixtures on the self-
7 healing capability of early-age concrete studied by means of permeability and crack closing tests”, *Construc-*
8 *tion and Building Materials*, 114, July 2016, pp. 447-457.
- 9 [71] Gupta, S., Al-Obaidi, S. and Ferrara, L.: “Meta-Analysis and machine learning models to optimize the effi-
10 ciency of self-healing capacity of cementitious materials”, *Materials*, 14, 2021, paper 4437, pp. 1-25,
11 <https://doi.org/10.3390/ma14164437>.
- 12 [72] Hesam Doostkami, Marta Roig-Flores, Pedro Serna, (2021), “Self-healing efficiency of Ultra High-Perfor-
13 mance Fiber-Reinforced Concrete through permeability to chlorides”, *Construction and Building Materials*,
14 310 art. n.125168.
- 15 [73] L. Ferrara, V. Krelani, M. Carsana, (2014), “A fracture testing based approach to assess crack healing of con-
16 crete with and without crystalline admixtures”, *Constr. Build. Mater.* 68, pp. 515–531,
17 <https://doi.org/10.1016/j.conbuildmat.2014.07.008>.
- 18 [74] ACI Committee 212, (2010), “212.3R-10 Report on Chemical Admixtures for Concrete”, American Concrete
19 Institute, 65 pages.
- 20 [75] Snoeck D. and De Belie N. (2019). Autogenous healing in strain-hardening cementitious materials with and
21 without superabsorbent polymers: an 8-year study. *Front. Mater.* 6:48, pp. 1-12.

Declaration of interests

Two of the authors are Guests Editors of the present special issue

The authors declare that they have no known competing financial interests or personal relationships that could have appeared to influence the work reported in this paper.

The authors declare the following financial interests/personal relationships which may be considered as potential competing interests.

Journal Pre-proof